



Cite this: DOI: 10.1039/d5np00083a

## Natural products with atypical atoms: unveiling structures, biosynthetic pathways, and bioactivities

Yeo Jin Lee,<sup>†a</sup> Hyeon-Jeong Hwang,<sup>ID †a</sup> Jungro Lee,<sup>†b</sup> Hyeon Seung Park,<sup>c</sup> Juwan Son,<sup>b</sup> Mohammad Seyedsayamdost,<sup>ID de</sup> Munhyung Bae,<sup>\*b</sup> Seoung Rak Lee<sup>\*a</sup> and Yun Kwon<sup>ID \*c</sup>

Covering: 1944–2025

Nature's biosynthetic repertoire extends far beyond conventional CHON(S) chemistry and encompasses a rare but diverse array of natural products that incorporate atypical elements such as arsenic, selenium, fluorine, iodine, boron, and vanadium. These metabolites reveal how living systems have evolved to harness atypical atoms through both enzyme-mediated and spontaneous chemical strategies. Biological C–F and Se–C bond formation, SAM-dependent arsenic methylation, and non-enzymatic boron complexation exemplify nature's ingenuity in overcoming extreme energetic or coordination constraints. Despite their scarcity, these compounds play critical ecological and physiological roles in detoxification and redox regulation (As, Se), defense, and signaling (F, I, B), and in some cases, sustain global biogeochemical cycles (Mo, V). Structurally, they exhibit exceptional chemical stability, redox versatility, and metal–ligand diversity. Functionally, these findings expand our understanding of enzyme evolution, chemical defense strategies, and symbiotic metabolism in both marine and terrestrial ecosystems. Recent genomic and biochemical advances have uncovered new families of atypical natural products and the specialized enzymes responsible for their formation. Taken together, these discoveries define the limits of biogenic chemistry and highlight promising avenues for sustainable biocatalysis and drug discovery, particularly in the fluorination, selenation, and boronation pathways that bridge biological and synthetic chemistry.

Received 26th November 2025

DOI: 10.1039/d5np00083a

rsc.li/npr

1. Introduction
2. Boron-containing natural products
  - 2.1. Tartrolons
  - 2.2. Boromycins
  - 2.3. Aplasmomycins
  - 2.4. Borophycin
  - 2.5. Hyaboron
  - 2.6. Autoinducer-2
3. Fluorine-containing natural products
  - 3.1. Fluorinated C2–C3 aliphatic carbonyl compounds
  - 3.2. Fluorinated fatty acids
  - 3.3. 4-Fluoro-L-threonine
4. Nucleocidin
  - 4.1. Arsenic-containing natural products
    - 4.1. Arsenobetaine
    - 4.2. Arsenosugars
    - 4.3. Arsenocholine
    - 4.4. Arsenolipids
    - 4.5. Arsenicin A
    - 4.6. Methylarsonous and dimethylarsinous natural arsenic products
5. Selenium-containing natural products
  - 5.1. Selenoneine
  - 5.2. Selenocysteine
  - 5.3. Ovoselenol
6. Iodine-containing natural products
  - 6.1. 3,6-Diiodocarbazole, methyl 2-iodobenzoate, and miur-aenamamide B
  - 6.2. Tasihalides A and B
  - 6.3. Phomopchalasins F and H
  - 6.4. Calicheamicins
7. Transition metal-containing natural products

<sup>a</sup>College of Pharmacy and Research Institute for Drug Development, Pusan National University, Busan 46241, Republic of Korea. E-mail: srlee17@pusan.ac.kr

<sup>b</sup>College of Pharmacy, Gachon University, Incheon 21936, Republic of Korea. E-mail: baemoon89@gachon.ac.kr

<sup>c</sup>BK21 FOUR Community-Based Intelligence Novel Drug Discovery Education Unit, College of Pharmacy and Research Institute of Pharmaceutical Sciences, Kyungpook National University, Daegu 41566, Republic of Korea. E-mail: yunkwon@knu.ac.kr

<sup>d</sup>Department of Chemistry, Princeton University, Princeton, NJ 08544, USA

<sup>e</sup>Department of Molecular Biology, Princeton University, Princeton, NJ 08544, USA

† These authors contributed equally to this review.



- 7.1. Vanadium-containing natural products
- 7.2. Molybdenum-containing natural products
8. Conclusions
9. Author contributions
10. Conflicts of interest
11. Data availability
12. Acknowledgements
13. References

## 1. Introduction

Natural products are among the richest sources of structurally diverse and biologically potent compounds. For more than half a century, the investigation of secondary metabolites from microorganisms, plants, and marine organisms has revealed an extraordinary repertoire of chemical architectures and bioactivities that profoundly influence modern medicine, agriculture, and biotechnology.<sup>1</sup> Despite this vast chemical diversity, the vast majority of natural products are composed of major biogenic elements, including carbon, hydrogen, nitrogen, and oxygen. Only a small fraction of metabolites contain atypical elements such as selenium, fluorine, iodine, or boron.<sup>2–5</sup> Nevertheless, these minor constituents are of considerable scientific importance, as their unusual atomic composition often leads to distinctive chemical reactivity, unique biosynthetic pathways, and specialized biological activities.<sup>2–5</sup>

The presence of atypical elements in natural products challenges conventional biosynthetic paradigms. In most microorganisms and plants, the intracellular concentrations of these elements are exceedingly low.<sup>6–8</sup> Furthermore, their distinct chemical properties, such as selenium's redox sensitivity, fluorine's high electronegativity, and boron's Lewis acidity, pose significant barriers to enzymatic processing. Nevertheless, nature has evolved enzymatic machinery capable of selectively incorporating these elements into complex organic scaffolds. The resulting compounds exhibit unique physicochemical characteristics, including altered lipophilicity, enhanced metabolic stability, and increased redox activity.<sup>3,9,10</sup> These features not only provide compounds with unusual biological effects but also broaden the diversity of natural products.

Although natural products containing chlorine or bromine have been thoroughly investigated, particularly in marine organisms, the biosynthesis and biological roles of those containing rare elements, such as iodine or fluorine, are far less understood. Elements such as selenium, arsenic, and boron, are often linked to basic or inorganic metabolism. However, recent studies have revealed their roles in the biosynthesis of complex secondary metabolites, endowing these compounds with unique structures and potent pharmacological activities.<sup>2–5</sup> These discoveries highlight that nature's biosynthetic capacity extends far beyond conventional CHNO-based chemistry. They also suggest that incorporating atypical elements into compounds may be a key evolutionary strategy for optimizing biological activities and ecological functions. From the perspective of natural product chemistry and drug discovery, secondary metabolites that incorporate atypical elements are

a particularly fascinating class of compounds. These compounds expand the accessible chemical space beyond that typically achieved using conventional synthetic methods. Their unique structures have motivated synthetic chemists to replicate or adapt the underlying biosynthetic principles to generate halogenated, selenylated, or boron-containing scaffolds with promising pharmacological potential.<sup>11–14</sup> Furthermore, recent advances in genome mining, metagenomics, and enzymology have begun to reveal the genetic and enzymatic foundations of these unusual biosynthetic pathways in microbes. These advances have enabled the identification of halogenases, selenoenzymes, and boron-utilizing enzymes that mediate rare element transformations under remarkably mild biological conditions.<sup>15–17</sup>

Despite these significant advances, an integrated understanding of the chemistry, biosynthesis, and biological functions of natural products containing atypical elements remains incomplete. Previous studies have focused on individual elemental classes, such as halogenated metabolites or selenium-containing compounds, without providing a unified perspective comparing their biosynthetic logic and structural diversity.<sup>3,11</sup> In light of the rapid expansion of this research field, a comprehensive analysis of how nature utilizes atypical elements such as selenium, fluorine, iodine, arsenic, and boron to expand its chemical diversity is both timely and necessary. In this review, we provide a comprehensive overview of the natural products that incorporate atypical elements. We discuss the structural diversity, elucidate the biochemical mechanisms by which these elements are selectively introduced, and examine their biological properties. Furthermore, we highlight the recent mechanistic and genomic studies that have unveiled the enzymatic foundations of these distinctive transformations. Finally, we offer perspectives on future research directions, emphasizing the potential of atypical element biosynthesis as a promising avenue for discovering novel bioactive compounds.

## 2. Boron-containing natural products

Although boron is a relatively rare element in the biosphere, it plays a significant role in certain natural products by forming unique coordination structures that contribute to their biological activity.<sup>18,19</sup> In particular, boron-containing natural products derived from microorganisms exhibit diverse bioactivities—including antibacterial, antiparasitic, and immunomodulatory effects—through the formation of distinctive boron–oxygen coordination structures known as boronate complexes, which are rarely observed in typical organic molecules.<sup>20–23</sup> These compounds have long remained elusive under conventional natural product screening methods; however, their presence is increasingly being identified with the advent of non-destructive analytical techniques such as <sup>11</sup>B nuclear magnetic resonance (NMR) spectroscopy.<sup>5</sup> This section provides a systematic overview of the known boron-containing natural products of microbial origin, focusing on their chemical structures, biosynthetic pathways, and biological activities.



## 2.1. Tartrolons

Following the general features of microbial boron-containing natural products outlined above, the tartrolon family (Fig. 1) is introduced first because it provides one of the most biosynthetically resolved macrodiolide-type boronate examples and thus serves as a representative blueprint for the shared assembly logic discussed in the remaining subsections. Among boron-containing natural products of microbial origin, the tartrolon family has attracted particular attention for its diverse biological activities and unique biosynthetic mechanisms. The first example of this group, tartrolon B (**1**), was initially isolated from *Sorangium cellulosum*.<sup>24</sup> Subsequent discovery of tartrolon C (**2**) and tartrolon E (**3**) from *Streptomyces* species further expanded the structural diversity of this class.<sup>25,26</sup> Although tartrolon A and tartrolon D are structurally related members of the tartrolon family, they do not contain boron; therefore, this section focuses on the boron-containing congeners **1–3**. These compounds are characterized as boron-coordinated macrodiolides, in which two symmetrical polyketide-derived monomeric units are joined to form a large macrocyclic ring.<sup>27</sup> Each monomeric unit consists of an extended alkyl chain and multiple oxygen functionalities, including hydroxyl groups.<sup>28</sup> These units are linked through ester bonds at both termini, forming a dimeric macrodiolide ring that exhibits an inherent structural symmetry, distinguishing it from conventional macrolides that typically arise from a single continuous polyketide chain.

Based on genomic analysis and structural homology studies, the core framework of tartrolon compounds is synthesized *via* a *trans*-acyltransferase (*trans*-AT) type I polyketide synthase (PKS) system.<sup>29</sup> Unlike conventional modular PKS systems, *trans*-AT PKSs lack integrated AT domains within each module; instead, discrete, *trans*-acting AT enzymes supply the appropriate extender units to the individual modules in a non-collinear fashion. The biosynthetic process is initiated from a D-lactate-derived starter unit, followed by the iterative incorporation of acetate and malonate building blocks to elongate the polyketide chain. During this process, tailoring domains such as ketoreductase (KR), dehydratase (DH), and enoyl reductase (ER) operate in a module-specific manner to control the oxidation state and stereochemistry of the intermediates. Together, these programmed reductive steps establish an oxygenation pattern and a stereochemical architecture that ultimately enables boron coordination in the mature scaffold.

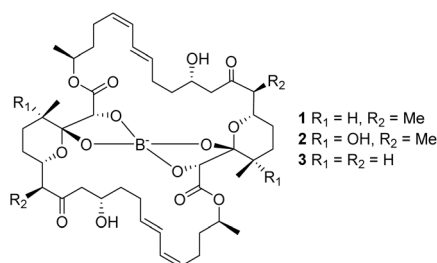


Fig. 1 The structures of compounds **1–3**.

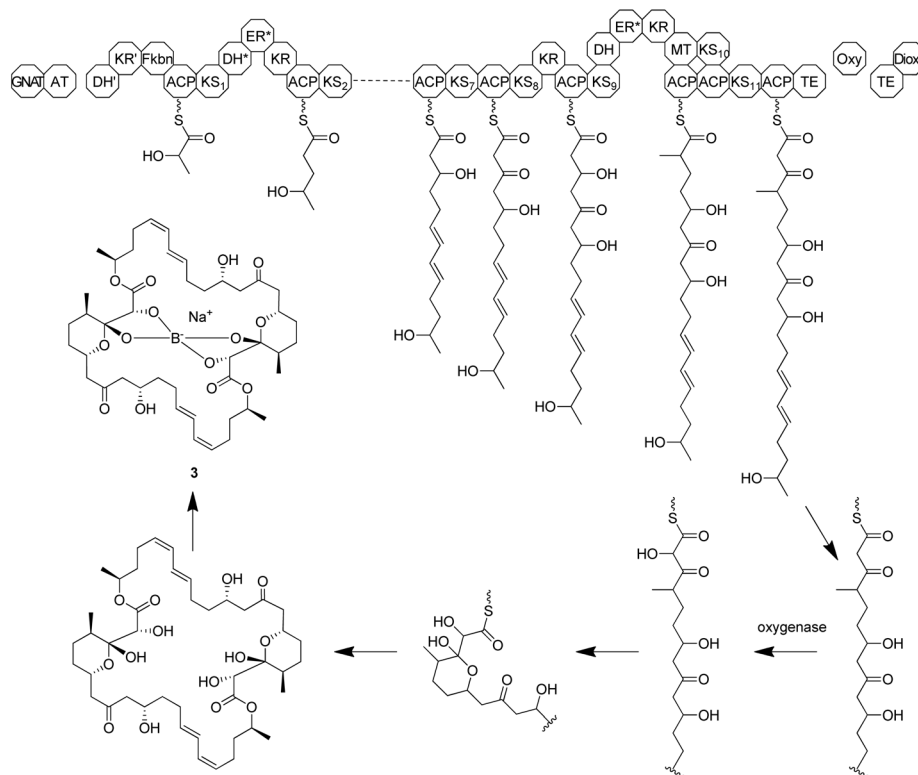
Upon completion of the chain elongation, the nascent polyketide is released by a thioesterase (TE) domain, during which two monomeric units are coupled *via* ester bonds to yield a macrodiolide ring. This TE-associated dimerization and macrodiolide formation is a defining step; it generates a symmetric (or pseudosymmetric) oxygen-rich macrocycle that contains multiple hydroxyl groups in a preorganized arrangement. All known members of the tartrolon family, including **1–3**, share this symmetrical or pseudosymmetrical macrodiolide scaffold.

Following macrodiolide ring formation, boron incorporation is believed to occur *via* a non-enzymatic chemical process. Environmental sources of boron, such as boric acid, spontaneously react with the four hydroxyl groups within the macrodiolide ring, leading to the formation of a stable central boronate complex (often described as a Böeseken-type borate/boronate complex, in which borate is held in tetrahedral coordination by four alcohol or  $\alpha$ -hydroxy oxygen donors). Notably, the natural conversion of tartrolon D to its boron-complexed analog **3** suggests that boron incorporation is not enzyme-mediated but may proceed irreversibly under appropriate environmental boron conditions.<sup>26</sup> This non-enzymatic boronation is interpreted as a selective late-stage modification that proceeds without perturbing the established stereochemical architecture of the macrodiolide. In the case of **2**, the structural diversity arises from an additional oxidation event at a specific position on the macrodiolide framework.<sup>29</sup> This modification is presumed to be mediated by a post-PKS tailoring enzyme (*i.e.*, a post-modification introduced after PKS-mediated scaffold assembly and release, such as site-specific oxidation), further expanding the chemical diversity within the tartrolon family.

Collectively, tartrolon biosynthesis is a multistep process that involves polyketide chain assembly, macrodiolide formation *via* TE domain-mediated dimerization (esterification), site-specific oxidation (when applicable), and late-stage boron complexation to yield boron-coordinated macrodiolide scaffolds. Importantly, this overall sequence—construction of a polyoxygenated polyketide scaffold, macrodiolide formation, and late-stage boronate complexation—reflects a recurring biosynthetic logic observed across several microbial boron-containing macrodiolides discussed in subsequent sections, with family-level differences primarily arising from the PKS type and domain/module organization, starter unit selection, and late tailoring reactions. Accordingly, compound **3** is among the most biosynthetically resolved examples of this class, and Scheme 1 is provided as a representative biosynthetic pathway illustrating the key steps of tartrolon E biosynthesis, including polyketide assembly, macrodiolide formation, and late-stage boron complexation.

Tartrolon B (**1**) exhibits antibacterial activity against gram-positive bacteria, including *Bacillus subtilis*, with minimum inhibitory concentrations (MICs) ranging from 0.3 to 1.56  $\mu\text{g mL}^{-1}$ .<sup>24</sup> Tartrolon C (**2**) exhibits insecticidal activity, with minimum emergent larvicide concentrations (MELCs) of 125 ppm against both *Spodoptera exigua* (beet armyworm) and *Heliothis virescens* (tobacco budworm).<sup>25</sup> This represented the first reported insecticidal chemotype within the tartrolon





Scheme 1 Proposed biosynthetic pathway of tartrolon E (3) as a representative example of boron-containing microbial macrodiolides.

family. Tartrolon E (3) exhibits nanomolar-level antiparasitic activity against *Plasmodium falciparum*, including both asexual and sexual blood stages.<sup>30,31</sup> Although it also shows cytotoxicity toward mammalian cells such as HepG2 (hepatocellular carcinoma) and L1210, its selectivity index exceeds 400, indicating significantly lower toxicity to host cells than to parasites.<sup>32,33</sup> Notably, compound 3 was also isolated from a symbiotic bacterium residing in shipworm gill tissues, suggesting a potential ecological role in protecting the host from apicomplexan parasites such as gregarines, highlighting its broader significance beyond pharmacological activity.<sup>29</sup>

## 2.2. Boromycins

Boromycin (4), originally isolated from *Streptomyces antibioticus*, is the first identified natural product known to contain

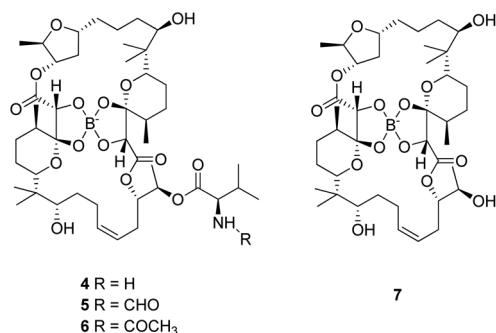


Fig. 2 The structures of compounds 4–7.

boron (Fig. 2).<sup>34</sup> Its structure featured a large 26-membered macrolactone ring incorporating multiple ether linkages and a central boron–oxygen coordination site. The seven ether bridges within the macrolide backbone facilitate the formation of a stable boronate complex.<sup>35</sup> Several structurally related derivatives have been reported, including *N*-formylboromycin (5), *N*-acetylboromycin (6), and desvalinylboromycin (7).<sup>36,37</sup> A notable structural characteristic of 4 was the incorporation of a *D*-valine-derived amino group on the macrolactone ring. This substituent, presumably introduced in the late stage of 4 biosynthesis, is the only nitrogen atom in its structure and highlights its hybrid origin by combining a polyketide scaffold with a peptidic component. In compounds 5 and 6, the amino group was modified *via* formylation and acetylation, respectively.<sup>36</sup>

The polyketide backbone of 4 was synthesized *via* a Type I modular PKS system, incorporating a total of 14 acetate/malonate extender units.<sup>38,39</sup> Six methyl groups are introduced by methionine-derived post-elongation methylation rather than by methylmalonyl-CoA extender incorporation.<sup>27</sup> Uniquely, the polyketide chain initiation is achieved through a three-carbon starter unit derived from glycerol, rather than the more typical propionate-based precursors.<sup>40</sup> Feeding experiments have confirmed *D*-valine as the direct biosynthetic precursor, and the retention of the  $\alpha$ -stereocenter indicated that the amino acid was incorporated without epimerization at the stereogenic center.<sup>27</sup> Upon completion of chain elongation, the polyketide intermediate is released by a TE domain and undergoes macrocyclization to yield the macrolactone ring. Although this



process follows a canonical modular PKS mechanism, post-tailoring addition of the D-valine moiety contributes to the structural uniqueness of the final molecule. Subsequent non-enzymatic reactions with boric acid have been proposed to generate characteristic boron–oxygen coordination sites (see Section 2.1).<sup>34,35,39</sup>

Following the structural elucidation of boromycin (4), additional derivatives, N-formylboromycin (5) and N-acetylboromycin (6), were identified, arising from formylation and acetylation of the terminal amino group, respectively.<sup>36</sup> Desvalinylboromycin (7) is a variant that lacks the D-valine moiety in its chemical structure.<sup>37</sup> These derivatives are supposed to arise from late-stage biosynthetic modifications and retain the characteristic boronate complex and polyketide backbone of 4. Collectively, these structural variants highlight the diversity introduced by terminal tailoring modifications within the biosynthetic framework of 4.

Compound 4 exhibits antibacterial activity against gram-positive bacteria, including *Mycobacterium tuberculosis*, with MICs ranging from 0.08 to 0.15  $\mu\text{M}$ .<sup>41</sup> Its mode of action involves functioning as a potassium ionophore, thereby dissipating the membrane potential. In addition, compound 4 displays nanomolar-level antiparasitic activity against protozoan pathogens such as *P. falciparum* and *Toxoplasma gondii*, and antiviral effects against HIV-1.<sup>42–44</sup> Although the biological activities of 5–7 have not yet been reported, they are likely to exhibit similar pharmacological properties due to their close structural resemblance to 4.

### 2.3. Aplasmomycins

The aplasmomycin family (Fig. 3) represents a distinctive group of boron-containing natural products characterized by a linear polyketide-like framework and a central boronate complexation motif. This class was first reported in *Streptomyces griseus* SS-20, with aplasmomycin A (8) being the initially isolated compound.<sup>45</sup> Subsequently, two derivatives, aplasmomycin B (9) and aplasmomycin C (10), were identified in the same strain.<sup>46</sup> All three compounds share an identical macrodiolide backbone but differ in their substitution patterns as a result of post-PKS modifications.

Compound 8 represents the prototypical member of its class and features a symmetrical macrodiolide backbone composed of 40 carbon atoms, in which a central boron atom forms a highly stable boronate complex through coordination with four hydroxyl groups.<sup>47</sup> Although the overall framework

resembles that of conventional polyether macrolides, compound 8 lacks the peptidic side chain commonly found in boromycin, distinguishing it structurally and biosynthetically.<sup>39</sup> Compounds 9 and 10 are acetylated derivatives of 8, arising through post-modifications.

The assembly of the polyketide-derived macrodiolide scaffold and the general late-stage boron complexation logic are consistent with the recurring framework summarized in Section 2.1. Notably, aplasmomycin biosynthesis is distinguished by the use of a glycerol-derived three-carbon starter unit (also observed for boromycins).<sup>48</sup> Experimental interconversion of debor-aplasmomycin to aplasmomycin in the presence of boric acid further supports the idea that boronation occurs after macrodiolide formation *via* a non-enzymatic or weakly enzyme-assisted process.<sup>49</sup> Compounds 9 and 10 are believed to arise through late-stage acetylation of hydroxyl groups following boronate complex formation, which may be enzyme-mediated *via* specific acetyltransferases or occur under culture conditions.

Aplasmomycin A (8), a boron-containing ionophore, exhibits antibacterial activity against gram-positive bacteria such as *Staphylococcus aureus* and *B. subtilis*, with MICs ranging from 0.78 to 3.12  $\mu\text{g mL}^{-1}$ .<sup>45</sup> It also shows *in vivo* antimalarial efficacy in *Plasmodium berghei*-infected mice, where oral administration significantly reduces parasitemia and improves survival. Aplasmomycin B (9), a monoacetylated derivative, shows lower antibacterial activity than 8; this change has been discussed in relation to the altered hydrogen-bonding capacity and steric effects around the boron coordination site,<sup>46</sup> with MICs against *S. aureus* and *B. subtilis* ranging from 4.2 to 125  $\mu\text{g mL}^{-1}$ . In the membrane-based assays, 9 retains its ionophoric activity for potassium transport at levels comparable to those of the parent compound. By contrast, aplasmomycin C (10), a diacetylated analog, shows reduced antibacterial activity in an agar disk diffusion assay, with relative activities of <5–6.3 (relative to aplasmomycin at 500  $\mu\text{g mL}^{-1}$ ), and low activity in potassium ion transport assays. This loss of bioactivity is likely due to the disruption of the boron coordination environment and reduced flexibility of the macrodiolide scaffold caused by dual acetylation. Further elucidation of the biosynthetic steps and their impact on structure–activity relationships is essential to advance the chemical and biological understanding of this unique family of boron-containing macrodiolides.

### 2.4. Borophycin

Borophycin (11) is a boron-containing natural product isolated from the cyanobacterium *Nostoc linckia* and features a symmetric macrodiolide scaffold composed of two identical monomers (Fig. 4).<sup>50</sup> Each monomer contains functional groups such as ketones, esters, ketals, multiple ether linkages, and hydroxyl moieties. The monomers are connected by two key interactions: each diol segment coordinates to a central boron atom to form a borate ester, and additional ester bonds link the monomers, completing the macrodiolide structure. This architecture yields a disc-shaped ionophore structure with a hydrophilic core defined by an oxygen-rich borate

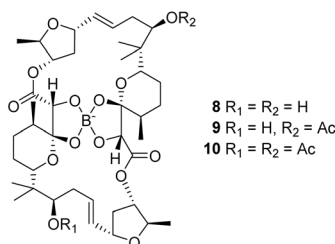


Fig. 3 The structures of compounds 8–10.



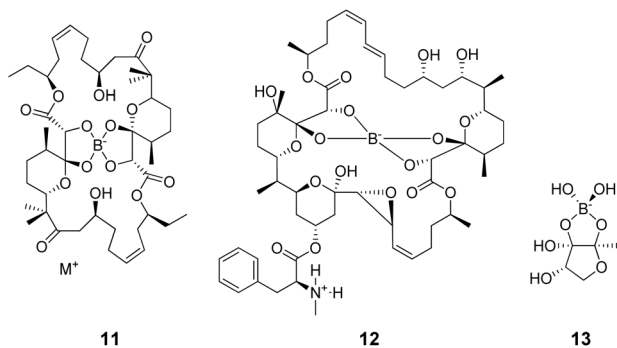


Fig. 4 The structures of compounds 11–13.

coordination sphere and a hydrophobic periphery composed of alkyl side chains. These structural features strongly suggest potential ionophoric properties of **11**.

The biosynthetic pathway of **11** is inferred to follow the polyketide route. Feeding experiments indicate that its carbon skeleton is assembled from acetate-derived C2 units with methyl groups derived from methionine<sup>50</sup> and that the C3 starter unit appears to originate from an acetate–methionine combination rather than propionate. After the chain release, dimerization is proposed to form the macrodiolide scaffold, followed by late-stage non-enzymatic boron complexation (see Section 2.1).

In terms of bioactivity, compound **11** exhibits cytotoxic activity against cancer cell lines.<sup>50</sup> It inhibits the growth of LoVo colon carcinoma and KB oral carcinoma cells with MICs of 0.066 and 3.3  $\mu\text{g mL}^{-1}$ , respectively. Compound **11** also shows antiviral activity in cell-based assays, inhibiting plaque formation by Herpes Simplex Virus type 2 (HSV-2) by 98% at 0.1 mg  $\text{mL}^{-1}$ .

## 2.5. Hyaboron

Hyaboron (**12**) is one of the most structurally and biologically distinct boron-containing natural products reported to date. This compound was first isolated from the myxobacterium *Hyalangium minutum* Hym3 and is notable for its asymmetrical architecture (Fig. 4).<sup>51</sup>

It comprises two chemically distinct polyketide-derived units l-linked by ester bonds, forming a macrodiolide framework. Each monomeric unit features a complex array of functional groups, including methylene, olefinic methine, ketone, ketal, and epoxide moieties. In particular, the presence of an epoxide between C-14 and C-15 and a six-membered ketal ring highlight the stereochemical complexity of the molecule. Although the biosynthetic pathway of **12** has not yet been fully elucidated, its assembly is presumed to follow the recurring framework summarized in Section 2.1, with a PKS-derived scaffold undergoing macrodiolide formation and late-stage boron complexation.

Compound **12** exhibits biological activities across multiple assays, including immunomodulatory, antimicrobial, cytotoxic, and antiparasitic effects.<sup>51</sup> In terms of its mode of action, compound **12** promotes the maturation and secretion of

interleukin-1 $\beta$  (IL-1 $\beta$ ) in both human peripheral blood mononuclear cells (PBMCs) and murine bone marrow-derived macrophages (BMDMs). This response is mediated by the activation of the NLRP3 inflammasome complex, triggered by intracellular potassium efflux. Compound **12** acts as a potassium ionophore, disrupting  $\text{K}^+$  homeostasis, thereby activating the cytosolic NLRP3 sensor protein and facilitating inflammasome assembly, culminating in caspase-1 activation and pro-IL-1 $\beta$  processing. In addition to its immunological effects, compound **12** shows antimicrobial activity against selected Gram-positive bacteria and fungi/yeasts. It inhibited *B. subtilis* DSM-10, *Micrococcus luteus* DSM-1790, and *S. aureus* DSM-346 with MIC values of 0.2, 0.4, and 0.8  $\mu\text{g mL}^{-1}$ , respectively, and showed activity against *Mucor hiemalis* DSM-2656, *Pichia anomala* DSM-6766, *Rhodotorula glutinis* DSM-10134, and *Schizosaccharomyces pombe* DSM-70572 with MIC values ranging from 0.8 to 8  $\mu\text{g mL}^{-1}$ .<sup>51</sup> It also exhibited antiparasitic activity at 1  $\mu\text{M}$ , inhibiting the growth of *Trypanosoma brucei rhodesiense*, *Trypanosoma cruzi*, *Leishmania donovani*, and *P. falciparum* by 100, 63, 95, and 100%, respectively.<sup>51</sup> Furthermore, compound **12** shows nanomolar-level cytotoxicity against several human cancer cell lines, with the strongest activity observed against A-431 (epidermoid carcinoma), A-549 (lung carcinoma), and KB-3.1 (cervix carcinoma) cells ( $\text{IC}_{50} = 13 \text{ nM}$ ), among the cell lines tested.<sup>51</sup> Taken together, these reports support **12** as a bioactive boron-containing scaffold, although further studies are required to establish its therapeutic potential and scope. Overall, the reported activities have been discussed in relation to the ionophoric modulation of intracellular ionic homeostasis, providing a mechanistic basis for future investigations.

## 2.6. Autoinducer-2

Autoinducer-2 (**13**) is a unique naturally occurring compound that exists as a boron-coordinated furanosyl borate diester (Fig. 4). It serves as a prototypical quorum-sensing (QS) signal that mediates inter-species communication among bacteria. The existence of **13** was first proposed in the mid-1990s during investigations into bioluminescence regulation in *Vibrio harveyi*, and it has since been identified as a broadly conserved signaling molecule produced by a wide range of gram-positive and gram-negative bacterial species.<sup>52,53</sup>

The biosynthetic pathway of **13** proceeds through a series of enzymatic reactions derived from the methionine salvage pathway, originating from S-adenosylmethionine (SAM).<sup>54</sup> This pathway initiates with the conversion of SAM into S-adenosylhomocysteine (SAH), which is subsequently hydrolyzed by 5'-methylthioadenosine/SAH nucleosidase (Pfs) to yield S-rib- osylhomocysteine (SRH). The key enzyme LuxS cleaves the C1–C2 bond of SRH, generating the sulfur-containing byproducts homocysteine and 4,5-dihydroxy-2,3-pentanedione (DPD). DPD serves as the immediate precursor of **13** and exists in aqueous solution as an equilibrium mixture of interconverting isomers (Scheme 2).

Some marine bacteria, such as *V. harveyi*, produce DPD, which reacts with boric acid when boron is readily available in the environment.<sup>53</sup> This reaction forms a structurally distinct



furanosyl borate diester that functions as a signaling molecule in QS pathways. The boron-coordinated form of **13** is recognized by the LuxP receptor and is biologically active. The conversion of DPD to boron-bound **13** occurs through a non-enzymatic chemical reaction and proceeds efficiently under marine or boron-rich environmental conditions. The crystal structure of the LuxP-**13** complex, in which boron is coordinated within the signal molecule, provides direct structural evidence for its role in AI-2 recognition. This structure demonstrates that borate complexation is essential for high-affinity binding to the LuxP receptor, thereby conferring receptor specificity and enabling precise inter-species QS.

Compound **13** functions as a key regulatory signal in bacterial QS networks. In *V. harveyi*, the boron-bound form of **13** specifically binds to the LuxP receptor, initiating downstream signaling cascades that modulate population-level behaviors such as bioluminescence, biofilm formation, and virulence factor expression.<sup>52</sup> In contrast, in *Escherichia coli*, **13** signaling occurs independently of boron complexation. The uncomplexed form of **13** is recognized by the LsrB receptor, which mediates transcriptional responses related to a wide range of physiological functions.<sup>54</sup> These differences in recognition indicate that **13** can be sensed through species-dependent pathways that vary with its boron-binding state. Accordingly, compound **13** was investigated as a target for developing quorum-sensing inhibitors (QSIs) with proposed applications to modulate microbial behaviors relevant to infection and ecological interactions. Further studies are needed to clarify the biological roles of **13** in QS-regulated communication and microbial community dynamics.

In addition to its established role in microbial QS networks, compound **13** has been investigated for its potential physiological effects on hosts. Although compound **13** does not appear to exhibit direct cytotoxic, anti-inflammatory, or antioxidant activity through conventional pharmacological mechanisms, recent studies suggest that it may influence host immune-related responses indirectly through host-microbiota interactions.<sup>55–57</sup> For example, elevated levels of **13** were observed in colorectal cancer (CRC) tissues, where they were associated with TNFSF9 signaling in tumor-associated macrophages and changes in CD3<sup>+</sup> T cell infiltration, consistent with

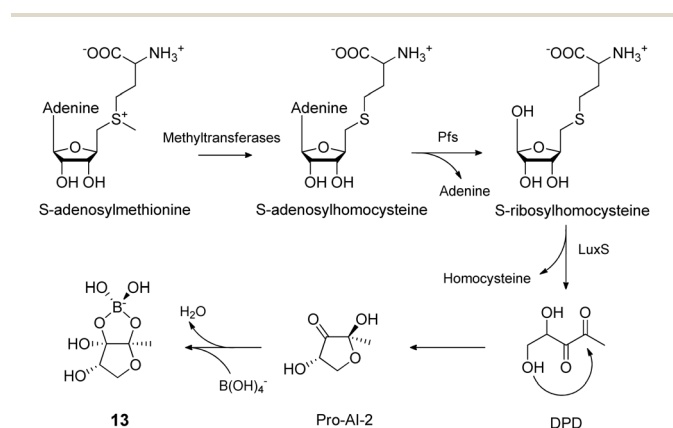
a potential immunomodulatory association in the tumor microenvironment.<sup>55</sup> Furthermore, exogenously administered **13** influences antibiotic-associated intestinal dysbiosis and markers of gut mucosal immunity, including epithelial barrier integrity and inflammatory cytokine levels.<sup>56</sup> Related effects have also been reported in experimental models of pulmonary inflammation, consistent with gut-lung axis crosstalk.<sup>57</sup> Overall, these reports suggest that **13** may contribute to host-microbe interactions and aspects of immune homeostasis, although the underlying mechanisms and physiological relevance remain to be established.

### 3. Fluorine-containing natural products

Fluorine occupies a paradoxical position in chemistry and biology. Despite its scarcity in natural systems, fluorine has become almost ubiquitous in synthetic chemistry and drug discovery, where a substantial fraction of pharmaceuticals, agrochemicals, and positron emission tomography (PET) imaging agents contain at least one C–F bond.<sup>58,59</sup> This prevalence reflects the unique ways in which fluorine can modulate acidity, lipophilicity, conformational preferences, and metabolic stability.<sup>59,60</sup> In contrast, fluorine is conspicuously under-represented in nature. Although thousands of chlorinated, brominated, and iodinated natural products have been characterized from marine organisms, terrestrial microbes, and plants, reflecting the widespread biological utilization of these halogens, only a small set of bona fide organofluorine natural products has been confirmed across all domains of life.<sup>60,61</sup> This disparity is particularly striking, given that fluorine is more abundant in the Earth's crust than bromine, chlorine, or iodine,<sup>60</sup> and it raises fundamental questions about the biochemical barriers to exploiting this element in living systems.<sup>60,61</sup>

At the heart of this puzzle lies the chemical intransigence of the C–F bond and bioinorganic properties of fluoride ions.<sup>60</sup> Fluorides are small, hard, and strongly hydrated, making them a poor nucleophile in aqueous solution; at the same time, the C–F bond is among the strongest single bonds in organic chemistry.<sup>60,61</sup> From the perspective of enzyme catalysis, both facts are problematic: the initial formation of C–F bonds is kinetically disfavored, and once formed, those bonds are difficult to remodel or cleave. It is, therefore, perhaps unsurprising that only a few specialized lineages have evolved the machinery to handle fluorine safely, developing not only fluorination enzymes but also resistance and detoxification strategies to avoid self-poisoning.<sup>60,61</sup>

Nevertheless, when biological systems engage with fluorine, the resulting metabolites are almost invariably highly potent and often exert pronounced ecological or pharmacological effects.<sup>60,61</sup> In this section, we review the known biosynthetic pathways, enzymatic machineries, and biological functions of naturally occurring organofluorine natural products, highlighting both their rarity and their disproportionate impact.



Scheme 2 Biosynthetic pathway of autoinducer-2 (**13**).



### 3.1 Fluorinated C2–C3 aliphatic carbonyl compounds

The first naturally occurring organofluorine compound identified was fluoroacetic acid (**14**) (Fig. 5), a simple C2 carboxylic acid.<sup>62</sup> This compound was initially recognized as the toxic principle of *Dichapetalum cymosum* and related *Dichapetalum* species in Africa. Subsequently, fluoroacetate (**15**) has been found in over 40 plant species across at least five genera on multiple continents, including *Dichapetalum* spp. (Africa),<sup>63</sup> *Gastrobium* and *Acacia* spp. (Australia), and others, many of which are notorious for poisoning livestock.<sup>64</sup> Compound **14** exhibits LD<sub>50</sub> values ranging from 0.05 to 10.0 mg kg<sup>-1</sup>.<sup>65</sup> Accumulation levels vary widely: leaves of *D. cymosum* can contain up to ~250 ppm of **15**, whereas the seeds of *Dichapetalum braunii* astonishingly reach ~7200–8000 ppm (0.7–0.8% dry weight) of **15**.<sup>66,67</sup> Young plant tissues and spring growth tend to have higher concentrations than mature tissues or off-season samples, reflecting the plants' strategic investment in chemical defense.<sup>68</sup>

Compound **15** is one of the most toxic natural plant metabolites. Synthetic sodium fluoroacetate (compound 1080) has been widely used as a rodenticide and predator control agent, exploiting the same toxicity mechanism as plants' natural defense mechanism with LD<sub>50</sub> ranging from 0.07 to 500 mg kg<sup>-1</sup>.<sup>68,69</sup>

Upon ingestion by herbivores, **15** is metabolized (*via* acetyl-CoA) to (2*R*,3*R*)-fluorocitrate, a suicide inhibitor of aconitase in the TCA cycle.<sup>68</sup> This leads to citrate accumulation, halting cellular respiration and causing convulsions and cardiac failure in grazing animals. The extreme potency of this toxin provides a clear evolutionary advantage to **15**-producing plants by deterring grazing by mammals and insects.

One historical anomaly is fluoroacetone (**16**), a volatile fluorinated ketone detected in an Australian plant (*Acacia georginae*) in the 1960s.<sup>70</sup> It was hypothesized as a byproduct of fluoroacetate metabolism (*via* malonyl-CoA condensation), but later investigations cast doubt on this finding.<sup>71</sup> Instead, **16** may have been misidentified; fluoroacetaldehyde (the hydrate of which can form **16** analogs in derivatization assays) is considered a more plausible intermediate in plant metabolism.<sup>72,73</sup>

As such, **16** is no longer considered a bona fide natural product.<sup>74</sup>

The enzymology of plant fluorometabolites remains unclear. No analog of the microbial C–F bond-forming enzyme (fluorinase) has been found in plants.<sup>75</sup>

Nonetheless, the widespread (if low-level) ability of plants to form organofluorines suggests a basic biosynthetic capacity in the plant kingdom. Intriguingly, trace amounts of **15** and fluorocitrate can be detected in some common crops and forage plants, such as tea, alfalfa, and clover, when grown in fluoride-rich conditions.<sup>76</sup> This observation suggests a potential, yet unconfirmed, capacity of plants to convert inorganic fluoride into organofluorine, although only certain species have evolved to accumulate high concentrations. In *D. cymosum*, **15** is predominantly synthesized in young leaves (which can contain >1000 ppm) and then translocated to other parts of the plant, such as older leaves or developing seeds.<sup>76</sup> Compound **15** may be temporarily stored or compartmentalized in leaf tissue adjacent to flowers and later mobilized—after fertilization—into seeds, where it is incorporated as fluoroacetyl-CoA into fatty acids.<sup>77</sup> Such spatial and temporal separation likely helps the plant avoid self-toxicity while still arming its seeds with a potent chemical defense for the next generation. It has also been speculated that when fluoroacetate is not required, plants may detoxify it by converting a fraction into volatile fluorinated compounds. For instance, seasonal declines in fluoroacetate levels correlate with increased emissions of volatile organofluorines, such as fluoroacetaldehyde, suggesting a possible detoxification pathway that vents fluorine as a gas.<sup>75</sup> However, direct *in vivo* evidence for this volatilization mechanism is lacking, and it remains a hypothesis.

Uncovering the plant enzymes responsible for fluoroacetate biosynthesis remains a key question. Given that no fluorinase homologs are present in these species, plants have likely evolved a completely different catalytic strategy for C–F bond formation, a tantalizing prospect for future discovery.<sup>75</sup>

### 3.2 Fluorinated fatty acids

The fluorinated fatty acids in *D. toxicarium* seeds appear to have similar defensive functions. Although these long-chain lipids are not acutely toxic,  $\beta$ -oxidation in predators releases fluoroacetate intracellularly. Thus, these compounds act as protoxins, extending the chemical defense to seed predators by generating lethal **15** within their own cells.<sup>76</sup>

Plant-derived fluoroacetate is frequently sequestered as sodium or potassium salts but may also be incorporated into complex lipids.<sup>62,68</sup> Early studies of *D. toxicarium* revealed a series of long-chain  $\omega$ -fluorinated fatty acids in seed oils, including 16-fluoropalmitic acid, 18-fluorooleic acid, 14-fluoromyristic acid, and 10-fluorocapric acid, as well as polyunsaturated analogs such as 18-fluorolinoleic acid.<sup>78</sup> A rare dihydroxy derivative, threo-18-fluoro-9,10-dihydroxystearic acid, likely arises from epoxy metabolism of 18-fluorooleate.<sup>79</sup> Subsequent studies identified additional  $\omega$ -fluorofatty acids, including 20-fluoroarachidic and 20-fluoroecosenoic acids, highlighting the metabolic versatility of these plants.<sup>78,80</sup>

These fluorinated lipids are biosynthesized using fluoroacetyl-CoA as a starter unit in fatty acid synthase, enabling chain extension from the two-carbon fluorinated precursor.<sup>77</sup> The restriction of such compounds to *Dichapetalum* species suggests a highly specialized evolutionary adaptation.

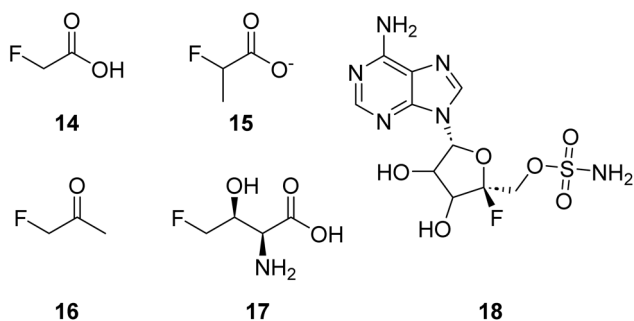


Fig. 5 The structures of compounds 14–18.



### 3.3 4-Fluoro-L-threonine

In the microbial world, fluorinated natural products are exceedingly rare and largely confined to Actinomycete bacteria.<sup>74</sup> The most studied example is *Streptomyces cattleya*, a soil bacterium remarkable for its ability to produce both **15** and 4-fluoro-L-threonine (**17**) as secondary metabolites (Fig. 5).<sup>81</sup> Compound **17** exhibits antibacterial activity against bacteria including *M. luteus*, with MICs ranging from 0.39 to 6.25  $\mu\text{g mL}^{-1}$ .<sup>82</sup> The discovery of fluorometabolites in *S. cattleya* was initially serendipitous—inorganic fluoride present as a trace impurity in growth media led to the unexpected biosynthesis of organofluorines, a phenomenon not seen in typical fermentations.<sup>81</sup> Intensive investigation showed that *S. cattleya* takes up fluoride and enzymatically incorporates it into **15** and **17**, releasing these compounds into the culture broth.<sup>81</sup> Notably, in a survey of 20 *Streptomyces* species, over half were found to absorb fluoride from the medium but none (in addition to *S. cattleya*) accumulated any fluorinated metabolite detectable by <sup>19</sup>F NMR.<sup>74</sup> This underscores the rarity of the fluorination trait even among Actinomycetes: the machinery for C–F bond formation is present in only a select few strains.

Genome mining and enrichment approaches have only identified a limited number of additional producers. *Streptomyces* sp. MA37, isolated from soil, harbors a fluorinase gene and synthesizes **15**, **17**, and (2*R*,3*S*,4*S*)-5-fluoro-2,3,4-trihydroxypentanoic acid, a shunt metabolite in the fluorothreonine pathway.<sup>83</sup> Bioinformatic surveys have also detected fluorinase homologs in *Actinoplanes* sp. N902-109 and *Nocardia brasiliensis*, exhibiting 80–87% sequence identity with the *S. cattleya* enzyme.<sup>59</sup> However, these organisms produce little or no fluorometabolites under standard laboratory conditions, suggesting pathway silencing or context-dependent regulation.<sup>59</sup>

### 3.4. Nucleocidin

Apart from fluorinase-pathway bacteria, the only other known microbial source of a fluorinated natural product is *Streptomyces calvus*, which produces nucleocidin (**18**, Fig. 5).<sup>84</sup> Nucleocidin is a rare, fluorinated antibiotic with a unique 4'-fluoro-5'-sulfamoyl adenosine scaffold. Unlike fluoroacetate-derived metabolites, its fluorine atom resides in the ribose moiety.<sup>84</sup> In addition, the C-5' sulfamate group represents an exceptionally rare functionality in natural products, also observed in its chlorinated analog, ascamycin.<sup>84</sup>

Nucleocidin exhibits potent activity against trypanosomes and bacteria, likely by inhibiting protein synthesis through interactions with tRNA synthetases or translation factors.<sup>85</sup> Despite early reports, *S. calvus* strains lost the ability to produce **18** for decades, creating a cryptic phenotype.<sup>86</sup> This mystery was resolved in 2015 when production was shown to depend on a *bldA*-encoded Leu-tRNA<sup>UUA</sup>. Restoration of this tRNA reactivates nucleocidin biosynthesis and enables detailed biochemical analyses.<sup>87</sup>

Microbial fluorometabolites function as chemical weapons in competitive environments. *S. cattleya* secretes **15** and **17**, which inhibit susceptible microorganisms by disrupting central

metabolism or amino acid utilization.<sup>81,83,88</sup> Resistance mechanisms protect the producer, conferring a strong ecological advantage.<sup>87</sup> Nucleocidin similarly serves as a potent antagonist, possibly deterring protozoan predators or competing microbes in soil habitats, and exhibits antibacterial activity against gram-positive bacteria, including *B. subtilis* with MICs around 200  $\mu\text{g mL}^{-1}$ .<sup>87,89</sup>

The extreme rarity of microbial fluorinated metabolites reflects both the scarcity of bioavailable fluoride and metabolic cost of fluorine chemistry.<sup>74</sup> Production typically requires millimolar fluoride concentrations that are rarely encountered in natural environments.<sup>75</sup> Nevertheless, fluoride-rich niches may support localized fluorine cycling. For example, fluoroacetate-degrading bacteria that possess dehalogenases coexist with producing organisms and use **15** as a carbon source.<sup>90</sup> This establishes a localized ecological loop involving toxin production and detoxification.

In summary, fluorinated natural products function as highly potent bioactive agents that enhance microbial fitness in specialized niches. Their scarcity reflects environmental constraints and biochemical complexity, yet their existence illustrates the remarkable evolutionary capacity of select microorganisms to exploit elements largely ignored by most life forms.<sup>74,75</sup>

## 4. Arsenic-containing natural products

Although arsenic is widely recognized for its toxicity, it also occurs naturally in diverse chemical forms, including organoarsenicals with distinctive structural features and biological functions.<sup>91</sup> Many arsenic-containing natural products originate from marine organisms and their associated microbiota, where arsenic is incorporated into stable metabolites or utilized as a bioactive scaffold.<sup>92</sup>

In biological systems, arsenic incorporation typically proceeds *via* methylation pathways from inorganic arsenate and arsenite, often mediated by SAM methyltransferases, followed by oxidative and reductive transformations.<sup>93</sup> Together, these processes generate a wide array of organoarsenic compounds. Importantly, arsenic speciation strongly dictates biological activity. Some organoarsenicals, such as arsenobetaine, are essentially inert, and inorganic arsenicals and certain reactive methylated species exhibit pronounced toxicity.

This section reviews the principal classes of naturally occurring organoarsenicals, emphasizing their chemical structures, biosynthetic pathways, and biological activities, with a focus on the comparative structure–activity relationships that underlie their diverse bioactivities.

### 4.1. Arsenobetaine

Arsenobetaine (**19**) is one of the most abundant naturally occurring organoarsenicals in marine food webs (Fig. 6). It was first identified in the mid-1970s in marine animals and is now known to be widespread in fish, crustaceans, mollusks, and macroalgae.<sup>94</sup> Structurally, **19** is a zwitterionic quaternary



arsonium carboxylate, consisting of an arsenic center (As<sup>[v]</sup>) bound to three methyl groups and a methylene group linked to a carboxylate moiety. This configuration generates an internal ion pair (As<sup>+</sup>/COO<sup>-</sup>) with no net charge, conferring high water solubility and exceptional chemical stability.<sup>95</sup> Notably, **19** represents the arsenic analog of the osmolyte glycine betaine, suggesting that it functions primarily as a benign storage and excretory form of arsenic in living organisms. Its zwitterionic nature minimizes its interactions with cellular macromolecules and contributes to its low biological reactivity.<sup>96,97</sup>

Biosynthesis of arsenobetaine proceeds *via* the oxidative demethylation of arsenocholine, which is a degradation product of algal arsenosugars.<sup>98,99</sup> Marine algae biosynthesize arsenosugars, which are subsequently metabolized by animals and associated microbiota to yield arsenocholine.<sup>100</sup> Oxidative demethylation of arsenocholine in host tissues then produces **19**. Isotope tracer experiments support this pathway and feeding studies have demonstrated the efficient conversion of arsenocholine into arsenobetaine in fish tissues.<sup>97</sup>

Thus, the formation of **19** represents the terminal step of a multistage biotransformation pathway involving the methylation, redistribution, and oxidative processing of inorganic arsenic. Through this sequence, reactive arsenic species are ultimately converted into chemically stable, biologically inert end products. Consistent with this role, arsenobetaine exhibits extremely low toxicity compared with that of inorganic arsenic species.<sup>101</sup> Its acute toxicity in mammals is orders of magnitude lower than that of arsenite (LD<sub>50</sub> in mice >10 000 mg kg<sup>-1</sup> for **19** versus ~34 mg kg<sup>-1</sup> for arsenite), and it is rapidly excreted unchanged without further bioactivation.<sup>93</sup>

In addition to its detoxification function, **19** acts as a compatible solute in microorganisms, enhancing tolerance to osmotic and thermal stress.<sup>100</sup> This dual role highlights arsenobetaine as both a metabolic sink for arsenic and a physiologically beneficial osmolyte.

#### 4.2. Arsenosugars

Arsenosugars constitute a diverse family of arsenic-containing ribofuranosides that are primarily found in marine algae, including brown, red, and green macroalgae, as well as in marine invertebrates that graze on algal biomass.<sup>93</sup> Their core structure consists of a 5-deoxyribose sugar (ribofuranose) linked glycosidically to a dimethylarsinoyl moiety. Structural diversity arises from substitutions at the 2', 3', and 5' positions, giving rise to glycerol, sulfate, phosphate, and sulfonate arsenosugars.<sup>93,102</sup> For example, a common arsenosugar contains a 2'-*O*-glycerol substituent, whereas others possess 2'-*O*-sulfate or related functional groups.<sup>103</sup>

Biosynthesis begins with the uptake of inorganic arsenate by algae, followed by SAM-dependent methylation mediated by arsenic methyltransferases to generate dimethylarsinoyl intermediates.<sup>93</sup> These intermediates are subsequently enzymatically conjugated to ribose-derived backbones, yielding mature arsenosugars. Arsenosugars serve as important metabolic precursors for other organoarsenicals, including arsenocholine and arsenobetaine, upon degradation in the marine food chains.<sup>97,98</sup>

Arsenosugars generally exhibit low acute toxicity in mammals but are not biologically inert. In humans, ingested arsenosugars undergo partial biotransformation to more toxic metabolites, including dimethylarsinous acid (DMA(III), **20**), which is associated with chromosomal aberrations and is detected as a transient metabolic intermediate (Fig. 6).<sup>104</sup> Nevertheless, arsenosugars rarely cause acute poisoning, and seafood containing these compounds is typically safe for consumption.

Ecologically, arsenosugars appear to function primarily in arsenic detoxification and storage within algae.<sup>105</sup> Algae can reduce arsenic-induced physiological stress by converting inorganic arsenate, which can interfere with phosphate-dependent metabolism, into stable organoarsenic conjugates. Consequently, the pentavalent arsenic center embedded within the sugar framework renders arsenosugars a relatively benign reservoir of arsenic. However, their subsequent degradation in higher organisms can regenerate toxic species depending on their metabolic capacity.<sup>103</sup> This dual behavior highlights arsenosugars as central intermediates in marine arsenic cycling.

#### 4.3. Arsenocholine

Arsenocholine (**21**) is a quaternary arsonium compound that is structurally analogous to choline, with arsenic replacing the nitrogen atom of the choline moiety (Fig. 6). In compound **21**, a dimethylarsinoyl group is linked to the 2-hydroxyethyl substituent to yield trimethylarsinioethanol. This compound has been detected in a variety of marine organisms, including fish, shrimp, and mollusks.<sup>97</sup> Although arsenocholine is not typically a dominant arsenic species, it plays a central role as a metabolic intermediate linking arsenosugars and arsenobetaine during marine arsenic cycling.<sup>97</sup>

Arsenocholine primarily originates from arsenosugar degradation. When algae containing arsenosugars are consumed by marine animals or decomposed by microorganisms, the cleavage of the ribose moiety liberates arsenocholine.<sup>97</sup> This process is analogous to the generation of choline-containing metabolites from the breakdown of glycerolphosphorylcholine. Once formed, arsenocholine undergoes further metabolism; in particular, the oxidative removal of the terminal hydroxymethyl group from the ethanol side chain converts **21** into arsenobetaine (trimethylarsinioacetic acid).<sup>100</sup>

Consistent with its role as a metabolic intermediate, arsenocholine exhibits low acute toxicity comparable to that of arsenobetaine (**19**). It is highly water-soluble and is readily excreted by animals. In marine organisms, **21** likely functions as

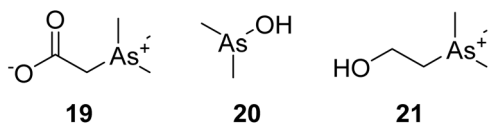


Fig. 6 The structures of compounds 19–21.



a transient storage or transport form of arsenic en route to more stable end products. Its structural similarity to choline prompted investigations into its potential interactions with choline-related metabolic pathways.<sup>104</sup>

Notably, arsenic-containing phospholipids (arsenolipids) with an arsenocholine head group have been identified, suggesting partial utilization of **21** in lipid metabolism.<sup>105</sup> However, no essential biological function has been established, and arsenocholine appears to function primarily as a transitory metabolite. Therefore, its presence in seafood is relevant for understanding arsenic speciation rather than its toxicological risk.

Overall, the quaternary arsonium structure of arsenocholine, comprising three methyl groups and one ethanol substituent, confers high chemical stability and low reactivity. Consequently, **21** does not readily interact with protein thiols or other toxicologically relevant targets, accounting for its minimal toxicity, similar to that observed for **19**.

#### 4.4. Arsenolipids

Arsenolipids are lipid-soluble organoarsenicals that were first identified in marine fish oils and are now known to occur widely in marine organisms and algae.<sup>106</sup> This class comprises several structurally distinct subclasses, including arsenohydrocarbons (AsHCs), which are long-chain hydrocarbons bearing dimethylarsinoyl functionality; arsenic-containing fatty acids (AsFAs) and related fatty alcohols, in which a dimethylarsinoyl group is attached to a carbon chain terminating in a carboxyl or hydroxyl group; and arsenophospholipids, such as arsenic-containing analogs of phosphatidylcholine.<sup>104,107</sup>

These arsenolipids exhibit substantial structural diversity. For example, AsHCs isolated from fish oils include species with molecular formulas such as C<sub>17</sub>H<sub>39</sub>AsO, representing arsenic-containing analogs of heptadecane, whereas arsenofatty acids span chain lengths from medium (C<sub>7</sub>–C<sub>12</sub>) to long (C<sub>14</sub>–C<sub>18</sub>) ranges.<sup>106</sup> A unifying structural feature is the presence of a dimethylarsinoyl moiety, which is typically connected to the lipid backbone through a carbon–oxygen linkage.

The biosynthesis of arsenolipids remains incompletely understood but is thought to involve the conjugation of dimethylarsinoyl units to lipid precursors. One proposed pathway involves the initial methylation of inorganic arsenic to form dimethylarsinate, followed by enzymatic attachment to pre-existing lipid scaffolds. Arsenosugars or arsenocholines produced in algae may serve as intermediates in this process. Garcia-Salgado *et al.* demonstrated that marine algae synthesize AsFAs, suggesting biochemical coupling of arsenic to fatty acid biosynthesis.<sup>110</sup> In the case of arsenophospholipids, an arsenocholine moiety likely replaces the native choline head group during phospholipid assembly.<sup>104,108</sup> Collectively, these observations suggest that organisms “mix and match” arsenic-containing units with conventional lipid frameworks, generating molecules that closely resemble endogenous lipids while incorporating arsenic.

The pronounced lipophilicity of arsenolipids distinguishes them from more common water-soluble arsenicals. Because of

their solubility in fats and oils, arsenolipids readily cross cellular membranes and accumulate in adipose tissues more efficiently than do arsenate or arsenosugars.<sup>109,110</sup> Several AsHCs and arsenofatty acids exhibit cytotoxicity to UROtsa and HepG2 cells, with IC<sub>50</sub> values of 8–13.5 μM.<sup>109</sup>

Arsenolipids also perturb lipid metabolism and have been suggested to contribute to dysregulation of the gastrointestinal microbiome when consumed in diets rich in fish oil.<sup>111</sup> From a structure–activity perspective, the incorporation of a dimethylarsinoyl group within a hydrophobic chain enables arsenolipids to function as molecular “Trojan horses,” transporting a reactive arsenic center into cellular membranes under the guise of a lipid. Partial metabolic processing can release inorganic arsenic or methylated oxo-arsenicals, thereby contributing to systemic arsenic exposure.<sup>111</sup>

Ecologically, arsenolipids may undergo biomagnification in marine food webs because of their preferential partitioning into fatty tissues. Therefore, regulatory agencies have noted that the presence of arsenolipids in seafood and fish oil supplements may pose distinct health risks, given their bioaccessibility and toxicity profiles.<sup>111</sup> In summary, the enhanced hydrophobicity and membrane permeability of arsenolipids confer elevated toxicological potential relative to water-soluble arsenicals, illustrating how the molecular context critically modulates the biological impact of arsenic.

#### 4.5. Arsenicin A

Arsenicin A (**22**) is a unique polyarsenic natural product that was isolated in 2006 from the New Caledonian marine sponge *Echinocalina bargibanti* (Fig. 7).<sup>110</sup> It represents the first poly-arsenic organic compound discovered in nature.<sup>110</sup> Its molecular formula, C<sub>3</sub>H<sub>6</sub>As<sub>4</sub>O<sub>3</sub>, and three-dimensional architecture are particularly remarkable. The molecule features an adamantane-type cage in which four arsenic atoms occupy positions analogous to the carbon vertices of adamantane, and three oxygen atoms bridge three of the six edges of the cage.<sup>110</sup> This arrangement generates a highly symmetrical tricyclic framework, often described as a tetraarsatricyclic structure, that resembles an inorganic arsenic oxide cluster embedded within an organic scaffold.

This compact As–O cage architecture is unprecedented among marine natural products and highlights nature’s capacity to construct complex arsenic–carbon frameworks.<sup>112</sup> In

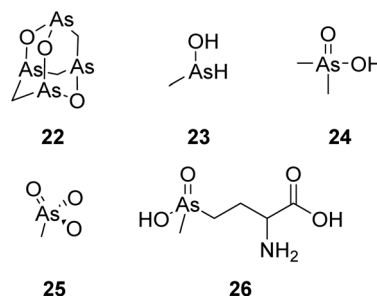


Fig. 7 The structures of compounds **22**–**26**.



22, each arsenic atom resides in a high oxidation state, commonly described as a mixed As(III)/As(V) system distributed across the cluster. The structure may be viewed conceptually as deriving from arsenic trioxide (As<sub>4</sub>O<sub>6</sub>), with three oxygen atoms replaced by methylene groups.<sup>113</sup> Owing to its asymmetric arrangement of arsenic and oxygen atoms, arsenicin A is chiral and has been resolved into enantiomers, although it is isolated from natural sources as a racemate.

However, the biosynthetic origin of 22 remains poorly understood. Current hypotheses suggest that it arises through coupling reactions involving inorganic arsenic species within the sponge or its associated microbiota.<sup>113</sup> One proposal suggests gradual assembly from smaller arsenic units, such as arsenite or methylarsenite, *via* oxidative coupling, potentially mediated by specialized enzymes or templating proteins.<sup>92,93,112,114</sup> Alternatively, the highly symmetric and dense As–O connectivity suggests that partially non-enzymatic processes, such as autocatalytic assembly in localized oxic microenvironments, may contribute.<sup>113</sup> Michelet *et al.* proposed that 22 could form through oxidative dimerization of arsenite to generate an As<sub>4</sub> intermediate, followed by structural rearrangement into the adamantane cage.<sup>113</sup> The involvement of unusual arsenic-related enzymes, including atypical arsenate reductases or peroxidases, remains an area of active speculation.<sup>114,115</sup> Collectively, these observations suggest that the production of such a complex arsenical reflects a highly specialized evolutionary adaptation potentially linked to chemical defense.<sup>114</sup>

Despite its inorganic-like characteristics, arsenicin A exhibits pronounced biological activity. It shows strong antibacterial activity against gram-positive bacteria, including *S. aureus* and *B. subtilis*, with potency in the low micromolar to sub-micromolar range.<sup>110,113</sup> Structurally related analogs, such as arsenicins B and C, in which one or two oxygen atoms are replaced by sulfur, exhibit activities comparable to those of standard antibiotics, including gentamicin.<sup>113</sup> The cage structure may also facilitate membrane intercalation, allowing the polar arsenic core to perturb membrane-associated proteins and promote oxidative damage.<sup>113</sup> Furthermore, redox cycling between arsenic oxidation states may contribute to the generation of reactive oxygen species (ROS).

In summary, the exceptional architecture of arsenicin A is closely associated with its potent antimicrobial activity and cytotoxicity. Its rigid cage structure and multivalent arsenic content confer substantial pharmacological activity while simultaneously requiring strict biological control of its production. Consequently, 22 likely functions as a highly specialized chemical weapon or deterrent, synthesized in limited quantities, to balance ecological advantage with self-protection.<sup>110,113</sup>

In addition, 22 shows moderate cytotoxicity against leukemia and solid tumor cell lines, including NB4, BxPC-3, MiaPaca-2, AsPC-1 and U87 cells, with IC<sub>50</sub> values in the sub-micromolar range (0.2–0.7 μM).<sup>112</sup> Notably, one study reported activity against promyelocytic leukemia cells at concentrations lower than those required for arsenic trioxide (Trisenox), highlighting its potential medicinal relevance.<sup>112</sup> Although the

precise mechanism of action remains unclear, the dense As–O cluster is likely central to its bioactivity. The proposed mechanisms include the induction of oxidative stress, strong binding to protein thiols and selenols, and the disruption of essential enzymatic pathways.<sup>113</sup>

#### 4.6. Methylarsonous and dimethylarsinous natural arsenic products

Methylated trivalent arsenicals, primarily methylarsonous acid (MMA(III), 23) and DMA(III) (20), occur sporadically in nature as transient metabolites and, in some cases, as deliberately produced bioactive compounds (Fig. 7).<sup>114</sup> Generally, these highly reactive species do not accumulate in organisms because they are unstable under oxygenated conditions.<sup>93</sup> Nevertheless, they play important roles in arsenic biogeochemistry and microbial interactions.<sup>114</sup>

In anaerobic or low-redox environments, such as animal gastrointestinal tracts, sewage sludge, and anoxic soils, microbial ArsM enzymes (As(III) SAM-dependent methyltransferases) convert inorganic arsenite to MMA(III) and subsequently to DMA(III).<sup>114</sup> Under oxic conditions, these trivalent methylarsenicals are rapidly oxidized to their pentavalent counterparts, dimethylarsinate (24) and methylarsonic acid (MMA(V), 25) (Fig. 7).<sup>101</sup> Consequently, detectable levels of MMA(III) and DMA(III) in natural samples are typically low and short-lived.<sup>114</sup>

Despite their ephemeral nature, certain microorganisms actively exploit trivalent methyl arsenicals as competitive weapons.<sup>114</sup> Several soil and gut bacteria, including *Streptomyces* species, can produce and excrete methylarsenite and related compounds to inhibit neighboring organisms.<sup>114</sup> These trivalent species are substantially more toxic than arsenite or arsenate, enabling producers to suppress competitors unless resistance mechanisms are present. Known defense systems include detoxification enzymes and efflux pumps encoded by genes such as *arsH*, *arsP*, and *arsN*.<sup>114</sup> This phenomenon has been widely described as microbial “chemical warfare.” In arsenic-rich environments, methylating microbes frequently outcompete non-methylators, supporting the view that ArsM evolved not only for detoxification but also for offensive ecological functions.<sup>114,115</sup>

In addition to simple methylarsenites, a limited number of specialized organoarsenicals have been identified in this category. A prominent example is arsinothricin (26), a broad-spectrum antibiotic discovered in *Burkholderia* species (Fig. 7).<sup>115</sup> Arsinothricin is a methylarsenical analog of glutamate that potently inhibits bacterial glutamine synthetase.<sup>114,115</sup> Although 26 is formally a pentavalent arsenic compound (2-amino-4-(hydroxymethylarsinoyl)butyrate), it is biosynthesized *via* a methylarsenite intermediate and similarly exploits the affinity of arsenic for biological ligands to exert antimicrobial activity.<sup>115</sup> These discoveries demonstrate that microbes can elaborate complex arsenic-based weapons beyond simple oxy-anionic species.

Trivalent methylarsenicals are among the most toxic arsenic species in biological systems. Their toxicity arises primarily from their strong reactivity toward thiols and other nucleophilic



functional groups in proteins.<sup>114</sup> MMA(III) and DMA(III) readily coordinate with cysteine residues, often forming stable arsenic-thiolate rings that inactivate enzymes.<sup>109</sup> They inhibit key metabolic pathways, including pyruvate dehydrogenase and other thiol-dependent systems, and disrupt cellular redox homeostasis.<sup>109</sup> DMA(III) displays markedly higher cytotoxicity than inorganic arsenite in human cells; in A549 cells, DMA(III) showed IC<sub>50</sub> values of approximately 14.1 μM, inorganic arsenite exhibited considerably higher IC<sub>50</sub> values of approximately 76.6 μM.<sup>116</sup> Comparative studies indicate a general potency order of MAs(III) > DMAs(III) ≈ As(III) ≫ As(V), with pentavalent species being far less toxic.<sup>117</sup>

This extreme reactivity explains why trivalent methylarsenicals rarely accumulate *in vivo*; the organisms that generate them must rapidly export or oxidize them into less harmful forms.<sup>114</sup> From an ecological perspective, the production of MMA(III) and DMA(III) strongly influences microbial community structure.<sup>114</sup> Only organisms possessing resistance mechanisms, such as ArsO oxidases, which convert MMA(III) to MMA(V), or ArsP/ArsK efflux systems, can persist under arsenic-selective pressure.<sup>101</sup> In rice paddies and other anaerobic habitats, microbial methylation and demethylation processes establish a dynamic equilibrium that prevents the long-term accumulation of these toxic intermediates.<sup>101</sup>

However, even transient exposure to low concentrations can exert disproportionate ecological effects, suppress sensitive species, and alter nutrient cycling. In summary, trivalent methylarsenicals exhibit a striking structure–activity relationship: adding one or two methyl groups to arsenite, while keeping arsenic in the +3 oxidation state, transforms a detoxification intermediate into a potent biological weapon.<sup>113,114</sup>

Arsenic-containing natural products exhibit an exceptionally broad spectrum of biological activities, ranging from virtually inert detoxification to highly potent antimicrobial and cytotoxic activities.<sup>103</sup> Arsenobetaine, arsenosugars, and arsenocholine (Sections 4.1–4.3) display minimal acute toxicity and primarily function as storage, transport, and excretory forms that mitigate arsenic-induced stress.<sup>92,97,99</sup>

In contrast, arsenolipids (Section 4.4) exhibit enhanced toxicological potential owing to their pronounced lipophilicity, which facilitates membrane permeation, cellular accumulation, and metabolic activation. These compounds disrupt mitochondrial function and lipid homeostasis, contributing to their cytotoxic and microbiome-altering effects.<sup>109</sup>

The most potent arsenic-derived bioactivities are observed for arsenicin A and trivalent methylarsenicals (Sections 4.5 and 4.6). Arsenicin A exhibits strong antibacterial and anticancer properties that are likely mediated by oxidative stress induction and thiol-binding mechanisms.<sup>112,113</sup> Trivalent methylarsenicals, including MMA(III) and DMA(III), are among the most toxic arsenic species in biological systems and function as chemical weapons in microbial competition by irreversibly inactivating enzymes.<sup>114</sup>

Collectively, these activities illustrate how biological systems exploit arsenic chemistry to generate metabolites spanning a continuum from detoxification reservoirs to highly specialized ecological and pharmacological weapons.

## 5. Selenium-containing natural products

Selenium is an essential trace element integral to numerous biological processes, including antioxidant defense, immune regulation, and redox homeostasis.<sup>118,119</sup> In biological systems, selenium is predominantly incorporated into selenoproteins such as glutathione peroxidases and thioredoxin reductases, which play pivotal roles in mitigating oxidative stress and maintaining cellular function. Microorganisms synthesize organoselenium compounds, often exhibiting unique structural features and potent biological activities.<sup>120</sup> Plants absorb selenium from the soil and incorporate it into amino acids such as selenocysteine and selenomethionine, which contribute to plant defense mechanisms and nutritional value.<sup>121</sup>

Selenium-containing natural products have attracted attention in drug discovery because of their diverse biological activities. Organoselenium compounds exhibit antioxidant, anti-inflammatory, anticancer, and antimicrobial properties. For example, methaneseleninic acid has anticancer activity and may enhance the efficacy of conventional chemotherapeutic agents. Given their structural diversity and potent bioactivity, selenium-containing natural products represent a valuable class of compounds for developing novel therapeutics. Ongoing research explores their biosynthetic pathways and molecular mechanisms, highlighting the chemical ingenuity of nature and potential for innovative drug development.<sup>122</sup>

### 5.1. Selenoneine

Selenoneine (27), a selenium-containing analog of ergothioneine, was first identified in 2010 as the predominant organic selenium compound in the blood and tissues of Pacific bluefin tuna (*Thunnus orientalis*) (Fig. 8).<sup>123</sup> Its microbial origin was later confirmed when *S. pombe* was shown to produce the compound when cultured in selenium-supplemented media. More recently, the complete biosynthetic pathway of 27 has been characterized in various microorganisms, including marine-derived strains such as *Amycolatopsis palatopharyngis* DSM 444832 and *Variovorax paradoxus* DSM 30034.<sup>124</sup> The biosynthetic pathway for 27 is encoded within a specialized gene cluster, *sen*, which encodes an unusual pathway wherein selenium is directly incorporated into a small-molecule natural product rather than into selenoproteins or selenonucleotides (such as Selenocysteine or Selenouridine). The gene cluster comprises three key genes, *senC*, *senB*, and *senA*, that orchestrate a series of reactions for the production of 27.<sup>125</sup>

The biosynthetic pathway begins with the activation of biologically inert selenide (HSe<sup>−</sup>) into a reactive selenium donor. In

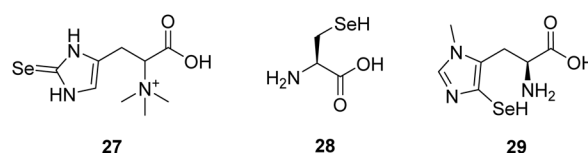


Fig. 8 The structures of compounds 27–29.



this initial step, SenC catalyzes the ATP-dependent conversion of selenide to selenophosphate (SeP), a reaction analogous to that of SeP synthetase SelD. The resulting SeP serves as a selenium donor in the downstream biosynthetic steps. In the second step, SenB catalyzes the coupling of SeP with UDP-sugar to generate 1-seleno- $\beta$ -D-glucose (SeGlc), a rare selenosugar containing a carbon-selenium (Se-C) bond. This reaction represents a previously uncharacterized Se-C bond-forming enzymatic process, establishing SenB as the first selenosugar synthase to be identified. SenB accepts a range of UDP-sugars (e.g., UDP-glucose, UDP-*N*-acetylglucosamine (UDP-GlcNAc), and UDP-GalNAc) as substrates, among which 1-seleno-*N*-acetylglucosamine (SeGlcNAc) serves as the primary intermediate involved in the biosynthesis of **27** (Scheme 3). In the final step, SenA, an oxidative enzyme homologous to EgtB in the ergothioneine biosynthetic pathway, catalyzes the coupling of SeGlcNAc and hercynine to produce hercynyl-SeGlcNAc selenoxide, a key intermediate en route to selenoneine. This intermediate is converted to **27** either under reducing conditions in the presence of dithiothreitol (DTT) or *via* spontaneous Cope elimination (Scheme 4). Notably, this transformation proceeds without the involvement of additional enzymes (such as EgtC or EgtE), thus providing a relatively simple route to the final product. This biosynthetic pathway is distinct from previously known selenium metabolic routes and represents a non-proteinaceous mechanism for selenium incorporation. This serves as an illustrative example of the biosynthesis of natural products bearing biologically rare Se-C bonds. Genomic analyses have revealed the widespread distribution of this pathway in diverse marine and terrestrial bacteria. This pathway may provide foundational information for developing selenium-based antioxidants, metal detoxifiers, and antimicrobials, thereby contributing to the exploration of the biosynthesis and bioactivity of natural products. In a human 3D epidermal model of functional melanocytes, selenoneine significantly suppressed melanin synthesis in a dose-dependent manner. At concentrations of 1.0 and 5.0  $\mu$ M, melanin levels were reduced to 39.7% and 23.0% of the control, respectively, demonstrating a more potent inhibitory effect than the positive control, arbutin.<sup>126</sup>

These findings highlight the strong anti-melanogenic potential of **27**. In the antioxidant evaluation, **27** shows stronger radical-scavenging activity than that of ergothioneine and Trolox in DPPH assays. Furthermore, treatment with **27** significantly reduces oxidative stress in *Caenorhabditis elegans* after 48 h, indicating that its antioxidant effects may involve modulating cellular signaling pathways beyond direct radical neutralization. In a zebrafish embryo model, **27** reduced

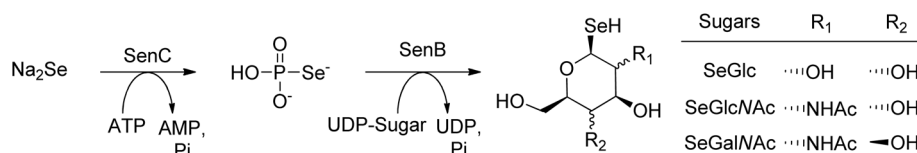
methylmercury (MeHg) toxicity and is involved in the conversion of MeHg to its inert form, mercury selenide (HgSe). Additionally, **27** competitively inhibits zinc-containing angiotensin-converting enzymes and suppresses melanin production in a human 3D epidermal model, indicating that it may exert skin-whitening effects by inhibiting tyrosinase activity.

In a colon cancer mouse model, the administration of tuna dark muscle extract containing **27** reduces both tumor number and size. In a non-alcoholic fatty liver disease (NAFLD) model, treatment with **27** decreases hepatic damage markers and attenuates lipid accumulation. These results suggested that **27** may provide physiological improvements in various diseases through its antioxidant and metabolic regulatory effects.<sup>126,127</sup>

## 5.2. Selenocysteine

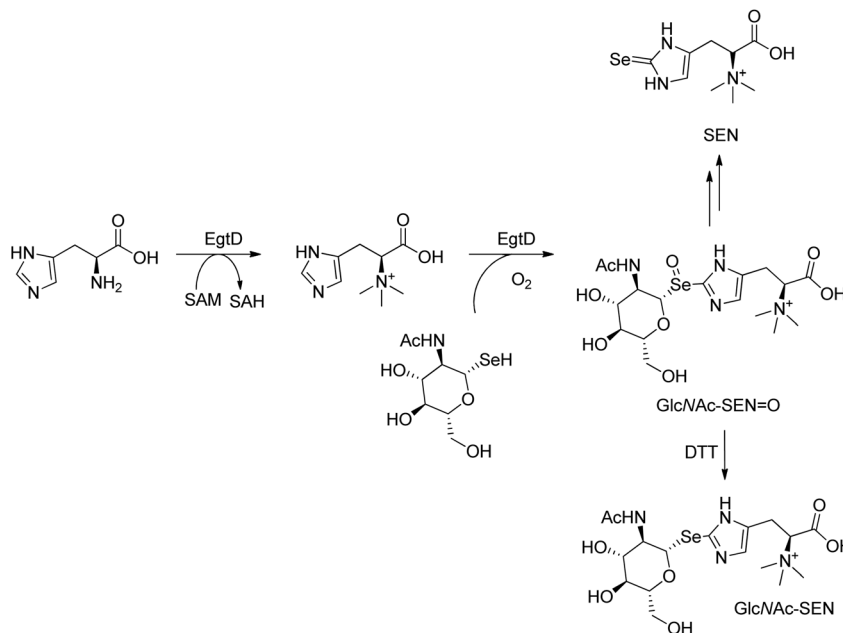
Selenocysteine (**28**) is a biologically essential amino acid structurally similar to cysteine but is differentiated by the substitution of sulfur with selenium (Fig. 8). The selenol group (-SeH) is highly reactive, which enables selenocysteine to play a critical catalytic role at the active sites of specific enzymes. Selenocysteine is incorporated into numerous selenoproteins that play pivotal roles in maintaining physiological homeostasis in diverse organisms.<sup>128,129</sup>

In bacteria, selenocysteine biosynthesis is a specialized process involving a unique set of genes and molecular machinery. The biosynthesis of **28** is unique and does not occur through standard codon-mediated amino acid incorporation. Although the UGA codon normally serves as a stop signal in protein translation, in the specialized mechanism for **28**, it is reinterpreted as a selenocysteine insertion codon. This process requires several components, including seryl-tRNA synthetase (SerS), which produces Ser-tRNA<sup>Sec</sup>; SelD, which synthesizes SeP; and SelA, which generates selenocysteyl-tRNA<sup>Sec</sup>. The resulting Ser-tRNA<sup>Sec</sup> is delivered to the ribosome by a dedicated factor, SelB, and this process is directed by a specific mRNA structure known as the selenocysteine insertion sequence (SECIS) element. Interestingly, certain microorganisms have evolved alternative mechanisms for selenocysteine biosynthesis. For instance, *Enterococcus faecium* ABMC-05, a lactic acid bacterium isolated from a traditional Mexican beverage, produces selenocysteine through a pathway independent of the canonical *selA* and *selD* genes.<sup>129</sup> Instead, this strain utilizes the *cysK* gene, which encodes cysteine synthase, suggesting a novel route for selenocysteine formation. This alternative mechanism underscores the metabolic diversity among microorganisms regarding selenium incorporation. These findings highlight the diversity of selenocysteine



**Scheme 3** SenC generates selenophosphate (SeP) from selenide, which is then used by SenB to synthesize selenosugars (SeGlc, SeGlcNAc, and SeGalNAc) from UDP-sugars.





**Scheme 4** SenA couples mercynine with SeGlcNAc to form mercynyl-SeGlcNAc selenoxide (GlcNAc-SEN = O), which spontaneously converts to selenoneine or is reduced to the corresponding selenoether.

biosynthetic pathways in microorganisms and the importance of selenocysteine-containing proteins in microbial physiology. Understanding these pathways can provide insights into selenium metabolism and its applications in biotechnology and medicine. In particular, studies on human glioma cells have shown that **28** induces apoptosis by targeting TrxR1, leading to excessive production of ROS, mitochondrial dysfunction, an imbalance in Bcl-2 family protein expression (upregulation of Bax and downregulation of Bcl-2), and activation of caspase-3 and cleavage of PARP1.<sup>130</sup> This apoptotic response was further linked to the disruption of the AKT and MAPK signaling pathways. Notably, antioxidant pre-treatment suppresses these effects, emphasizing the pivotal role of ROS in **28**-induced apoptosis. *In vivo* experiments using U251 glioma xenografts in mice confirmed that administering **28** significantly inhibited tumor growth, consistent with TrxR1-targeted oxidative damage.<sup>130</sup>

In *C. elegans*, **28** mimicked the effects of dietary restriction (DR), with lifespan extension requiring SKN-1 and accompanied by nuclear translocation of DAF-16 (the ortholog of mammalian FoxO). Consequently, treatment with **28** increased the mean lifespan from ~17.9 to 22.6 days.<sup>131</sup> Selenocysteine also alleviates stress induced by a high-glucose diet and delays amyloid- $\beta$ -induced paralysis, suggesting its potential neuroprotective effect in Alzheimer's disease models. Taken together, these findings indicate that selenocysteine functions not merely as a sulfur substitute but also as a regulator of redox homeostasis and apoptosis and may therefore contribute to processes relevant to cancer and neurodegenerative diseases.<sup>132</sup>

### 5.3. Ovoselenol

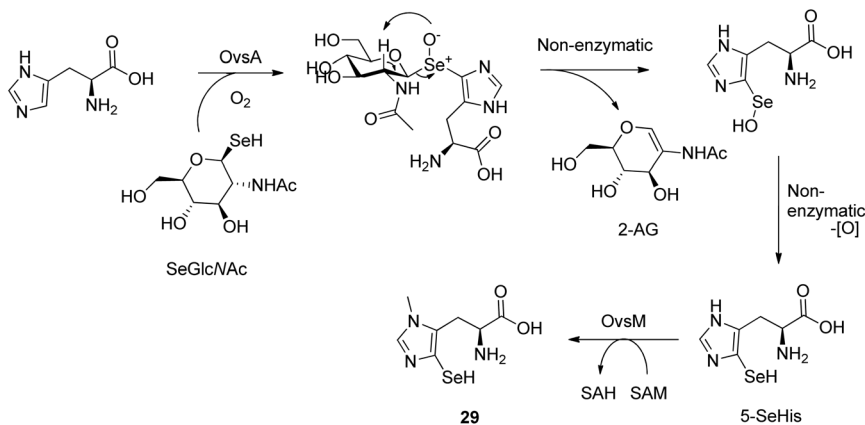
Ovoselenol (**29**) is a recently identified selenium-containing natural antioxidant belonging to the thio/selenoimidazole

(TSI) class of histidine derivatives (Fig. 8).<sup>133</sup> This compound plays a vital role in cellular defense mechanisms against oxidative stress and significantly broadens the scope of biological selenometabolites by introducing novel selenium-based bioactive functionalities. Compound **29** has a unique structure, in which selenium is directly bonded to the imidazole ring. This C–Se bond is rare in biological molecules and confers potent antioxidant properties to **29**. Although **29** shares structural similarities with other TSI-class antioxidants, such as ergothioneine and ovoidiol, the presence of selenium confers distinct chemical characteristics.<sup>120</sup>

The biosynthesis of **29** begins with histidine and proceeds through a sequence of enzymatic reactions that yield a TSI antioxidant featuring direct selenium incorporation (Scheme 5). The first step involves the formation of *N*-acetyl-1-seleno- $\beta$ -D-glucosamine (SeGlcNAc) by reacting selenium, activated *via* SeP, with sugar. This step is catalyzed by the enzymes SenC and SenB, following a pathway similar to that of the previously known selenosugar synthesis. Subsequently, the key enzyme, OvsA, a non-heme iron-dependent oxidase, introduces selenium from SeGlcNAc into the C-5 position of the imidazole ring of histidine. This leads to the formation of the intermediate 5-selenoxide, which is rapidly deglycosylated and reduced to 5-selenohistidine (5-SeHis). In the final step, the SAM-dependent methyltransferase OvsM methylates the imidazole ring of 5-SeHis to yield the final product, **29**. Although this pathway is mechanistically analogous to ovoidiol biosynthesis, the formation of the C–Se bond in **29** represents a unique biosynthetic feature, highlighting the biochemical diversity of selenium utilization in nature.<sup>133</sup>

In addition to its unique biosynthetic pathway, **29** is a newly identified microbial selenometabolite that features a C–Se bond. This structural feature contributes to its redox activity.





Scheme 5 Biosynthetic pathway of ovoselenol (29).

Electrochemical analysis revealed that **29** exhibits a reduction peak potential of  $-1.02$  V, which is more positive than that of **28** ( $-1.28$  V), suggesting its comparatively enhanced electron-donating capacity and possible relevance as an unusual redox-active selenium compound. Although compound **29** exhibits promising redox properties, its precise physiological function remains to be elucidated. However, further studies are required to investigate its potential involvement in redox regulation, transcriptional control, and metal stress responses. The identification of **29** adds to the growing chemical diversity observed in microbial selenium metabolism and underscores the need to further explore the functional roles of selenometabolites in nature.<sup>133</sup>

## 6. Iodine-containing natural products

Iodine-containing natural products are predominantly found in marine microorganisms, algae, and some invertebrates, in which iodine is incorporated into structurally diverse scaffolds.<sup>11,134</sup> These iodinated compounds exhibit a wide range of biological activities, including antimicrobial, anticancer, anti-inflammatory, and antioxidant properties, thereby significantly contributing to host defense and ecological adaptation in marine environments. Recent advances in halogenase enzyme characterization shed further light on the biosynthetic origin of iodine incorporation. In particular, flavin-dependent halogenases have been identified in marine actinobacteria and are responsible for the regioselective introduction of iodine into aromatic precursors under mild physiological conditions.<sup>135</sup> These enzymes are of increasing interest in biocatalysis and drug development because of their substrate specificity and environmental compatibility.<sup>136</sup>

Given their structural novelty and potent bioactivity, iodine-containing natural products represent an important frontier in marine natural product research, offering therapeutic potential for multiple diseases, including cancer, infectious diseases, and metabolic disorders. Continued exploration and characterization of these compounds will not only elucidate the functional roles of iodine in marine biosystems but also expand the repertoire of bioactive scaffolds for drug discovery.

### 6.1. 3,6-Diiodocarbazole, methyl 2-iodobenzoate, and miuraenamides

3,6-Diiodocarbazole (**30**) is a halogenated carbazole alkaloid isolated from the marine cyanobacterium *Kyrtuthrix maculans* (Fig. 9).<sup>137</sup> This compound has two iodine atoms in its carbazole core, which contribute to its unique chemical properties. The carbazole-based **30** exhibits antimicrobial activity, particularly against *B. subtilis*, a gram-positive bacterium. At a concentration of  $31.25 \mu\text{g mL}^{-1}$  ( $74.6 \mu\text{M}$ ), **30** demonstrated stronger inhibitory effects than did the reference antibiotic amoxicillin, which was only active at  $62.5 \mu\text{g mL}^{-1}$  ( $171.1 \mu\text{M}$ ).<sup>138</sup> Against *E. coli*, a gram-negative bacterium, **30** exhibited moderate activity, with inhibition observed at  $62.5 \mu\text{g mL}^{-1}$  ( $149.2 \mu\text{M}$ ), comparable to the activity of amoxicillin under the same conditions. In contrast, ciprofloxacin, used as a positive control, exhibited superior antibacterial activity with a minimum inhibitory concentration of  $3.9 \mu\text{g mL}^{-1}$  ( $11.8 \mu\text{M}$ ).<sup>138</sup>

Methyl 2-iodobenzoate (**31**) is a naturally occurring halogenated aromatic ester first isolated from the actinomycete *Streptomyces chartreusis* (Fig. 9).<sup>139</sup> It represents the earliest known example of a naturally produced iodinated volatile organic compound. As a volatile compound, **31** may play a role in microbial communication or chemical defense; however, its ecological and physiological functions remain unclear. Cultivation of *S. chartreusis* in GYM medium enriched with 2-iodobenzoic acid resulted in the detection of methyl 2-iodobenzoate. This finding indicates that *S. chartreusis* likely converts the

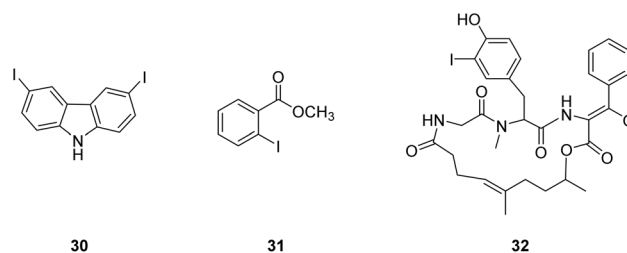


Fig. 9 The structures of compounds 30–32.



supplemented carboxylic acid precursor into a methyl ester through an efficient *in situ* methylation process.

Miuraenamides B (32) is a natural cyclic depsipeptide product isolated from the myxobacterium *Paraliomyxa miuraensis* (strain SMH-27-4) (Fig. 9).<sup>140</sup> This strain was isolated from a soil sample collected near the coast of the Miura Peninsula in Kanagawa Prefecture, Japan. Structurally, 32 belongs to a unique class of secondary metabolites featuring a macrocyclic ring composed of both peptide and ester linkages, which contributes to its structural rigidity and bioactivity. Miuraenamides B shares an identical core structure with miuraenamides A, with a structural difference in the substitution of bromine with iodine at the tyrosine residue.<sup>141</sup> Miuraenamides A is biosynthesized through a biosynthetic gene cluster consisting of two type I PKS genes (*miuA* and *miuB*), one non-ribosomal peptide synthetase (NRPS) gene (*miuC*), and four tailoring enzyme genes (*miuD–G*). The biosynthesis of miuraenamides A is initiated using acetyl-CoA as a starter unit, followed by iterative extensions with malonyl-CoA and methylmalonyl-CoA to form the polyketide backbone, after which L-alanine, brominated tyrosine, and methoxylated phenylalanine are sequentially incorporated *via* the NRPS modules. The resulting intermediate is then cyclized and released by the TE MiuF, and the FAD-dependent halogenase MiuG catalyzes the bromination of free L-tyrosine to introduce the specific bromotyrosine moiety in miuraenamides A. MiuG catalyzes the iodination of the L-tyrosine moiety during the biosynthetic pathway of miuraenamides B. In an anti-*Phytophthora* screening experiment using the paper disk diffusion method, 32 exhibited strong antimicrobial activity, inhibiting the growth of the phytopathogen *Phytophthora capsici* at the very low concentration of 0.025 µg per disc.<sup>142</sup>

## 6.2. Tasihalides A and B

Tasihalides A (33) and B (34) are structurally unprecedented iodinated diterpenes isolated from a marine cyanobacterium belonging to the genus *Symploca* and an unidentified red alga, respectively (Fig. 10).<sup>143</sup> These compounds are characterized by a distinctive polycyclic cage-like framework and are the only known naturally occurring iodine-containing diterpenes. The exceptional structural features and rarity of iodine-containing diterpenes highlight their chemical and biological significance. As unique halogenated secondary metabolites, these compounds provide valuable insights into the chemical diversity of marine natural products and help expand their repertoire. Compounds 33 and 34 are biosynthetically derived through the halogenation-triggered cyclization of oxidized cembrane-type diterpenes. In both compounds, iodine and bromine are regioselectively incorporated at the C-16 and C-4 positions, respectively, indicating a highly specific, possibly enzymatically controlled, halogenation mechanism.<sup>143</sup>

Compounds 33 and 34 are derived from cembrane diterpenes, and their biosynthesis primarily involves halogenation and cyclization reactions. In the initial step, the cembrane diterpenes react with halogens (iodine or bromine) and undergo halogenation. After the halogen attachment, the compound forms an additional ring structure *via* an

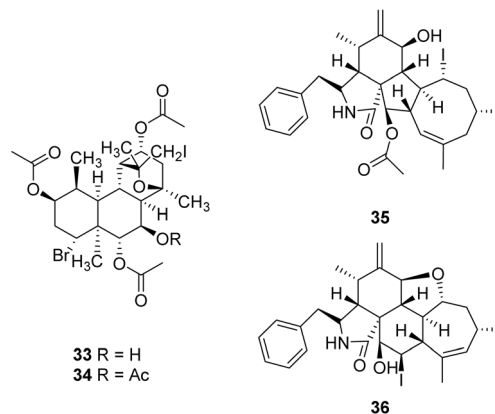


Fig. 10 The structures of compounds 33–36.

electrophilic reaction. This process begins with oxygenated cembrane diterpenes and is significantly mediated by haloperoxidase, an enzyme derived from red algae that promotes ring formation using halogens. The resulting ring structures yield unique iodinated diterpenes 33 and 34. It is more likely that 33 and 34 originate from red algae rather than cyanobacteria. Marine cyanobacteria predominantly produce bioactive compounds *via* the polyketide and non-ribosomal peptide pathways, often yielding modified amino acid structures. By contrast, peptide- or acetogenin-like structures have rarely been reported in cyanobacteria. In particular, diterpene compounds are scarcely found in cyanobacteria but are frequently detected in red algae, particularly those of the genus *Laurencia*. Considering these biosynthetic distribution characteristics, 33 and 34 are more likely to originate from red algae.<sup>143</sup>

## 6.3. Phomopchalasins F and H

Phomopchalasin F (35) and H (36) were isolated from a marine plant-derived fungal strain, *Phomopsis* sp. QYM-13, cultured in a medium supplemented with 3% potassium iodide (Fig. 10).<sup>144–147</sup> The cytotoxic activities of these compounds were evaluated by measuring IC<sub>50</sub> (50% inhibitory concentration) values against a panel of human cancer cell lines, including MDA-MB-435 (breast carcinoma), HepG2 (hepatocellular carcinoma), A549 (lung carcinoma), MDA-MB-231 (breast carcinoma), and SNB19 (glioblastoma), as well as the non-cancerous Vero cell line (African green monkey kidney). Compound 35 exhibited cytotoxicity only against the Vero cell line, with an IC<sub>50</sub> value of 29 µM, while showing low IC<sub>50</sub> ± SD values of 47 ± 1, 47 ± 3, 33 ± 1, 43 ± 2, >50, and 29 ± 1 µM, respectively, against the other cell lines. Compound 35 showed cytotoxic activity only against the Vero cell line at 39 ± 1 µM and exhibited limited activity (>50 µM) against all other tested cell lines. These results indicate that both compounds exhibit particularly high cytotoxicity against Vero cells.<sup>147</sup>

## 6.4. Calicheamicins

Calicheamicins (Fig. 11) are a class of highly potent antitumor antibiotics produced by *Micromonospora echinospora* ssp.



*calichensis*, a species within the genus *Micromonospora*.<sup>148</sup> These compounds were first discovered in the mid-1980s from caliche clay soils in Texas. Notably, the incorporation of sodium iodide into the fermentation medium led to the biosynthesis of iodine-containing calicheamicin analogs, highlighting the influence of halide supplementation on structural diversification during microbial secondary metabolism. Subsequently, various derivatives have been isolated and studied, with calicheamicins  $\alpha_2^I$  (37),  $\alpha_3^I$  (38),  $\beta_1^I$  (39),  $\gamma_1^I$  (40), and  $\delta_1^I$  (41) representing major isomers, each possessing unique structural and biological characteristics.

Calicheamicins are composed of three key components: an enediyne core, a trisulfide-containing trigger moiety, and a unique oligosaccharide unit.<sup>149</sup> These structural elements are biosynthesized through a series of highly orchestrated enzymatic steps in *M. echinospora* ssp. *calichensis*. The central enediyne core, which confers a potent DNA-cleaving activity, is biosynthesized by an iterative type I PKS. This enzyme modulates the formation of a highly strained macrocyclic structure by incorporating conjugated triple and double bonds, which are further modified by associated tailoring enzymes to afford a characteristic 10-membered enediyne framework. Following core formation, multiple rare sugar residues are appended by glycosyltransferases in a stepwise manner, facilitating specific recognition and binding to the minor groove of the DNA. The final biosynthetic step involves the incorporation of a trisulfide

moiety derived from cysteine, which functions as a molecular “trigger” that activates the enediyne for DNA strand scission. In addition, calicheamicins contain an iodinated orsellinic acid moiety; however, the timing of iodine incorporation during biosynthesis has not yet been clearly established. This modular biosynthetic strategy yields calicheamicin analogs with remarkable cytotoxicity and therapeutic potential.<sup>150</sup> Although the calicheamicin derivatives exhibit strain-dependent variability, they show potent antibacterial activity against a wide range of bacteria. Compounds 37, 38, 39, and 41 showed MICs ranging from 0.06 to 0.5  $\mu\text{g mL}^{-1}$  against key pathogenic strains, including *E. coli*, *Klebsiella pneumoniae*, *Enterobacter* sp., and *Citrobacter* sp.<sup>148</sup> Notably, compounds 37–41 exhibited exceptional antibacterial potency against *S. aureus*, *S. epidermidis*, *S. faecalis*, *M. luteus*, and *B. subtilis*, with MICs as low as 0.0005  $\mu\text{g mL}^{-1}$ , effectively inhibiting bacterial growth at concentrations markedly lower than those of conventional antibiotics.<sup>148</sup>

Iodine-containing isomers show enhanced activity and are expected to play a significant role in various therapeutic applications, including cancer treatment. Compound 40, in particular, induces double-stranded DNA breaks, leading to cell death and antitumor efficacy. Through mechanisms involving cytotoxicity and DNA damage induction, it exerts a potent anti-neoplastic effect, notably causing strong cytotoxicity and showing antitumor activity through mechanisms such as NAD depletion and poly (ADP-ribosylation) activation.<sup>150</sup>

## 7. Transition metal-containing natural products

Transition metal-containing natural products comprise metabolites and biogenic complexes that incorporate redox-active metals such as vanadium and molybdenum, which play direct functional roles through metal–ligand coordination and electron transfer, in contrast to the nonmetal and metalloid elements discussed above.<sup>151</sup> In living systems, transition metal-containing natural products occur predominantly as protein-bound cofactors, whereas discrete small-molecule metabolites remain relatively uncommon but chemically distinctive. By stabilizing unconventional coordination environments, these metals expand the structural and functional space, enabling redox catalysis and group-transfer chemistry and contributing to processes such as storage, signaling, and chemical defense.<sup>152</sup> Recent advances in natural product discovery, analytical workflows, and purification strategies have enabled more confident elucidation of the structures and origins of these transition metal-containing metabolites. Ongoing research continues to clarify their biosynthetic origins, structural features, and biological functions, thereby providing information for informing future applications in chemical biology and natural-product-inspired discoveries.

### 7.1. Vanadium-containing natural products

In the Earth's crust, vanadium constitutes the 21st most abundant element, and in seawater, it's the 2nd most abundant

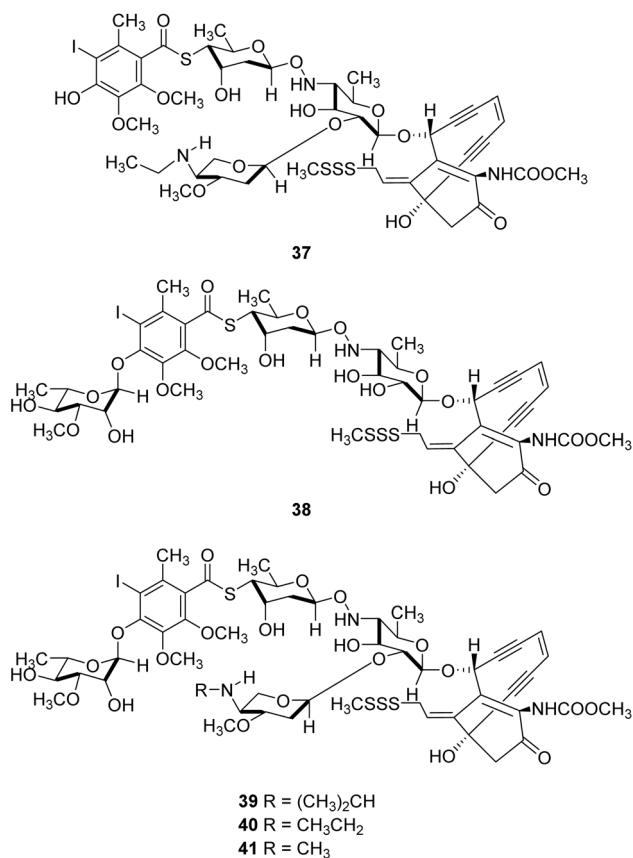


Fig. 11 The structures of compounds 37–41.



transition metal.<sup>153</sup> In biological and environmental systems, vanadium predominantly exists as pentavalent vanadate ( $\text{VO}_4^{3-}$ )—forming pH-dependent species (e.g.,  $\text{HVO}_4^{2-}$  and  $\text{H}_2\text{VO}_4^-$ ) that mimic phosphate in signaling—and as tetravalent vanadyl ( $\text{VO}^{2+}$ ), produced by vanadate reduction under reducing conditions and readily forming stable protein complexes for metal transport and storage.<sup>154,155</sup> However, despite extensive research, the precise mechanism and biological role of vanadium in vertebrates (and hence humans) remain to be elucidated,<sup>156</sup> but various vanadium compounds have been explored as potential anti-diabetic agents and evaluated for a variety of additional therapeutic indications.<sup>155,157</sup>

Vanadium-containing natural products (Fig. 12) include a single non-protein small molecule, amavadin (**42**),<sup>158</sup> along with two broad classes of vanadium-binding macromolecules: vanabin (**43**), which are cytoplasmic storage and carrier proteins identified in ascidian blood cells,<sup>159</sup> and functional enzymes such as vanadium-dependent haloperoxidases (**44**) and vanadium-dependent nitrogenases (**45**).<sup>160</sup> Given their structural diversity and potent bioactivities, vanadium-containing natural products represent promising leads for new drug development and therapeutic applications. The following section summarizes known vanadium-containing natural products, with emphasis on their origins, structural features, and biological functions.

Amavadin (**42**), originally isolated from fly agaric (*Amanita muscaria*),<sup>162</sup> is the first and only non-proteinaceous small-molecule natural product known to incorporate vanadium. Electron paramagnetic resonance (EPR) spectroscopy established vanadium's +4 oxidation state in amavadin, and the full structure was subsequently reported a year later.<sup>161</sup> Subsequently, studies employing EPR, infrared (IR) spectroscopy, and other analytical techniques led to further revisions of the proposed structures.<sup>162–164</sup> Definitive elucidation of amavadin's structure was achieved in 1987 through X-ray crystallography and NMR spectroscopy.<sup>165,166</sup> Its structure features a vanadium(IV) center in a rare non-oxo, octacoordinate environment chelated by two fully deprotonated (*S,S*)-*N*-hydroxyimino-(2,2′)-dipropionate (HIDPA) ligands. Each tetradentate HIDPA ligand binds *via* one oximate N–O donor and two carboxylate O donors, yielding an overall  $[\text{V}(\text{HIDPA})_2]^{2-}$  complex anion with  $C_2$

symmetry.<sup>167</sup> Amavadin (**42**) exists in two helical isomeric forms,  $\Delta$ -amavadin and  $\Lambda$ -amavadin, depending on the right- or left-handed orientation of the  $C_2$ -symmetric HIDPA ligands around the vanadium(IV) center. NMR and CD spectroscopy have shown that natural product **42** exists in solution as an approximately 1 : 1 mixture of the  $\Delta$ - and  $\Lambda$ -isomers.<sup>168</sup> Until now, no structurally related derivatives of **42** have been reported, and its biosynthetic pathway in *A. muscaria* remains uncharacterized.

Although no pharmacologically relevant biological activity has been demonstrated for **42**, several studies have reported its redox-mediated catalytic properties *in vitro*. Amavadin promotes the oxidation of thiols such as cysteine and glutathione, both in the absence and presence of hydrogen peroxide, exhibiting peroxidase- and catalase-like behavior.<sup>165,169</sup> It also facilitates per-oxidative halogenation and hydroxylation of organic substrates under oxidative conditions.<sup>169</sup> Electrochemical studies revealed that **42** catalyzes thiol oxidation *via* a mechanism consistent with Michaelis–Menten kinetics.<sup>170</sup> Additionally, **42** catalyzes the oxidation of methane to acetic acid under mild conditions in the presence of peroxodisulfate and trifluoroacetic acid.<sup>171</sup> Although the physiological relevance of this transformation remains unknown, such reactivity supports its potential role as a redox mediator in fungal metabolism.

Although **42** remains the only known vanadium-containing small molecule, vanadium more commonly occurs in living organisms as part of macromolecular complexes. Among these are vanabins (**43**) identified in the ascidian *Ascidia sydneiensis samea*<sup>172</sup> and fan worm *Pseudopotamilla ocellata*.<sup>173</sup> Vanabins with molecular masses of 12.5, 15, and 16 kDa were found in the cytoplasm of vanadocytes using immunodetection with specific antibodies.<sup>172,174</sup> Subsequent studies advanced the molecular characterization of vanabins. Biochemical analyses demonstrated their high selectivity for V(IV) over other metals,<sup>162</sup> and molecular cloning revealed two isoforms, vanabin 1 and vanabin 2, capable of binding 10 and 20 vanadyl ions, respectively.<sup>175</sup> Structural studies using NMR spectroscopy provided the first three-dimensional model<sup>176</sup> and later uncovered a cysteine-rich folding pattern, unlike that of any known metalloprotein.<sup>177</sup> Despite extensive structural and biochemical characterization, the physiological function of vanabins appears to be limited to intracellular vanadium storage and transport within vanadocytes.<sup>162,175,176,178</sup>

In addition to serving as a storage protein, vanadium functions as a catalytic enzyme cofactor. The best-studied examples are vanadium-dependent haloperoxidases (**44**), which employ vanadate covalently bound to a histidine residue to catalyze the oxidation of halides by hydrogen peroxide.<sup>177,179</sup> These enzymes have been identified in marine algae, such as *Ascophyllum nodosum* and *Corallina officinalis*,<sup>177,180</sup> as well as in terrestrial fungi and lichens,<sup>181</sup> where they participate in the biosynthesis of diverse halogenated metabolites. Vanadium-dependent nitrogenases (**45**) represent another class of catalytic enzymes found in certain diazotrophic bacteria such as *Azotobacter vinelandii*.<sup>182</sup> Unlike canonical molybdenum nitrogenases, the vanadium-dependent form contains a V–Fe cofactor and is

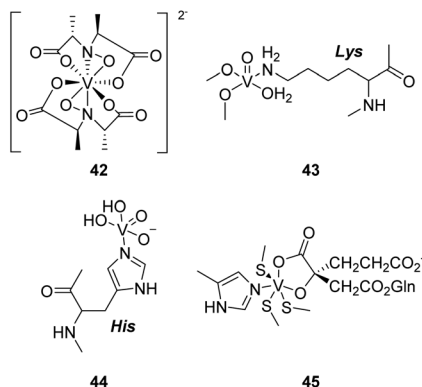


Fig. 12 The structures of compounds **42**–**45**.



capable of reducing dinitrogen to ammonia under molybdenum-limited conditions<sup>182,183</sup> while also exhibiting higher activity toward alternative substrates such as CO and CN<sup>-</sup>.<sup>184</sup> Together, these vanadium enzymes illustrate how organisms exploit the unique redox versatility of vanadium to catalyze key oxidative and reductive transformations in nature.

## 7.2. Molybdenum-containing natural products

Molybdenum is an essential transition metal in a wide range of living systems, from bacteria to higher eukaryotes.<sup>185</sup> Its unique redox flexibility enables catalytic functions indispensable to nitrogen, sulfur, and carbon metabolism.<sup>186</sup> These include processes such as nitrate reduction, sulfite detoxification, and purine metabolism.<sup>187</sup> In living systems, molybdenum is predominantly present as the soluble molybdate anion (MoO<sub>4</sub><sup>2-</sup>), which represents the biologically accessible form of the element.<sup>188</sup>

For catalytic activity, molybdenum is incorporated into cofactors that serve as integral components of diverse metalloenzymes.<sup>189</sup>

Molybdenum-containing natural products (Fig. 13) are exclusively represented by protein-bound cofactors rather than small molecules. The molybdenum cofactor (Moco, **46**) is widely distributed in nature<sup>190</sup> and supports the catalytic activity of enzymes such as xanthine oxidase,<sup>191</sup> sulfite oxidase,<sup>192</sup> and nitrate reductase.<sup>193,194</sup> In contrast, the structurally distinct iron–molybdenum cofactor (FeMoco, **48**) serves as the catalytic core of nitrogenase, mediating the biological reduction of dinitrogen to ammonia.<sup>195</sup> Given their essential catalytic roles, molybdenum-containing natural products represent important targets for biomedical research and the development of novel therapeutics.<sup>189</sup> This section highlights current knowledge of their occurrence, structural organization, and catalytic functions across diverse biological systems. The Moco (**46**), a pterin-based metallocofactor, was first identified in the early 1970s through studies of molybdoenzyme-deficient mutants in organisms such as *Neurospora crassa*, which revealed that multiple enzymes require a shared molybdenum-containing cofactor.<sup>186,196</sup> Structurally, **46** is constructed on a conserved molybdopterin (**47**) scaffold, featuring a tricyclic pyranopterin core that coordinates the molybdenum center through an

enedithiolate ligand. Its structure was initially elucidated by chemical degradation studies, which established the pterin-based framework and sulfur ligation pattern, and was later corroborated by crystallographic analyses of molybdenum-dependent enzymes.<sup>197–199</sup> Through this coordination environment, **46** enables a broad spectrum of redox transformations, most prominently hydroxylation and oxo-transfer reactions. Moco-dependent enzymes mediate essential transformations in carbon, nitrogen, and sulfur metabolism, including purine catabolism, sulfite detoxification, and nitrate reduction.<sup>187</sup> In higher eukaryotes, these catalytic functions are indispensable for maintaining metabolic homeostasis, whereas deficiencies in **46** biosynthesis result in severe and often lethal metabolic disorders.<sup>200–202</sup>

The FeMoco (**48**) represents a structurally and functionally distinct form of molybdenum used in biology. Unlike the universally distributed pterin-based Moco, **48** is exclusively associated with nitrogenase enzymes, where it serves as the catalytic core for the biological reduction of dinitrogen to ammonia.<sup>203,204</sup> Crystallographic analyses revealed its unique cluster architecture, [(MoFe<sub>7</sub>S<sub>9</sub>C)-homocitrate], consisting of a molybdenum center coordinated by homocitrate and a carbide-bridged Fe–S cluster.<sup>205,206</sup> This elaborate metallocluster exemplifies one of the most complex cofactors known in nature and confers the exceptional reducing power of nitrogenase.<sup>207</sup> Beyond dinitrogen reduction, **48** also displays reactivity toward alternative substrates such as CO and CN<sup>-</sup>, highlighting its remarkable catalytic versatility.<sup>183,184</sup> Together, Moco (**46**) and FeMoco (**48**) exemplify the diversity of molybdenum-containing natural products, highlighting how fundamentally distinct architectures enable molybdenum to serve versatile catalytic functions in biology.

## 8. Conclusions

Natural products containing atypical elements, such as arsenic, selenium, fluorine, iodine, boron, molybdenum, and vanadium, represent some of the most striking demonstrations of the chemical adaptability of nature. Once considered biochemical outliers, these metabolites collectively reveal that life has evolved multiple strategies to incorporate atypical atoms into organic frameworks, extending the boundaries of biological chemistry far beyond the traditional CHON(S) repertoire.

From a biosynthesis perspective, these unusual atoms are introduced *via* remarkably diverse mechanisms. Arsenic and selenium are incorporated through SAM-dependent methylation and SeP-mediated routes, respectively, whereas fluorine enters the metabolism *via* a fluorinase-catalyzed nucleophilic substitution reaction—the only known biological C–F bond-forming process. In contrast, boron and iodine are frequently installed *via* non-enzymatic or halogenase-assisted processes, and transition metals such as molybdenum and vanadium are incorporated into sophisticated cofactors that mediate essential redox transformations. These contrasting strategies, ranging from enzymatic precision to spontaneous coordination,

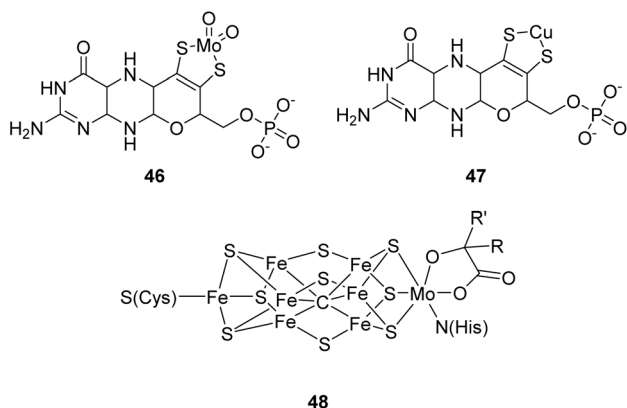


Fig. 13 The structures of compounds **46**–**48**.



underscore the biochemical ingenuity of nature in overcoming the physicochemical constraints of rare elements.

Despite their rarity, atypical natural products have pivotal ecological and physiological roles. Arsenobetaine and arsenosugars act as detoxification and storage forms in marine food webs, whereas selenium metabolites such as selenoneine and selenocysteine provide antioxidant protection and redox regulation across organisms. Fluorinated metabolites, such as fluoroacetate and 4-fluoro-L-threonine, function as potent antifeedants and enzyme inhibitors, reflecting the use of fluorine for chemical defense. Iodinated compounds, particularly marine metabolites, such as tasilhalides and miuraenamides, exhibit pronounced antimicrobial and cytotoxic effects, highlighting the ecological and pharmacological significance of halometabolites. Boron macrolides such as boromycin and tartrolon E function as ionophores with activity against *M. tuberculosis* and *P. falciparum*, whereas molybdenum and vanadium cofactors underpin central metabolic and nitrogen-fixing reactions that are fundamental to global biogeochemical cycles.

These examples reveal convergent evolutionary strategies: (i) chemical stabilization of reactive atoms through coordination (B, Mo, and V); (ii) controlled redox modulation enabling detoxification or signaling (Se and As); and (iii) electrophilic halogenation as a means of defense or metabolic diversification (F and I). These patterns reflect the adaptive value of element-specific chemistry for ecological survival and inter-species competition. Importantly, several of these pathways, particularly those involving halogenases, methyltransferases, and selenium- or boron-handling enzymes, demonstrate that life can exploit even the most energetically demanding reactions by evolving specialized enzymatic architectures and cofactor systems.

In addition to their natural context, these metabolites hold substantial promise for biotechnological applications and drug discovery. Fluorinase from *S. cattleya* has inspired biofluorination platforms for the synthesis of fluorinated pharmaceuticals. Boron-containing macrolides have served as leads for next-generation antibiotics, and the Sen pathway of selenoneine biosynthesis provides a model for engineering Se–C bond-forming enzymes. Similarly, the structural logic of iodine- and arsenic-containing metabolites provides new scaffolds for developing anticancer and antimicrobial agents. Together, these systems exemplify how knowledge of element-specific biosynthetic logic can guide the rational design of bioinspired catalysts and therapeutics.

Integrating genomics, metalloproteomics, and metabolomics will likely reveal additional families of rare element natural products hidden in unexplored microbiomes and marine symbioses. Coupled with advances in cryo-EM, isotope-enabled tracing, and machine learning-based pathway prediction, future studies can elucidate how these elements are selected, activated, and integrated by living systems. Ultimately, exploring atypical element biosynthesis illuminates the outer limits of biological chemistry, where the inorganic and organic worlds converge, and paves the way toward sustainable

biotechnologies that harness the same molecular ingenuity that has been refined for millions of years.

## 9. Author contributions

Yeo Jin Lee: investigation, data curation, and writing – original draft. Hyeon-Jeong Hwang: investigation, data curation, and writing – original draft. Jungro Lee: investigation, data curation, and writing – original draft. Hyeon Seung Park: investigation and data curation. Juwan Son: investigation and data curation. Mohammad Seyedsayamdost: writing – review & editing. Munhyung Bae: conceptualization, data curation, supervision, writing – original draft, writing – review & editing, and funding acquisition. Seoung Rak Lee: conceptualization, data curation, supervision, writing – original draft, writing – review & editing, and funding acquisition. Yun Kwon: conceptualization, data curation, supervision, writing – original draft, writing – review & editing, and funding acquisition.

## 10. Conflicts of interest

There are no conflicts to declare.

## 11. Data availability

No new data were generated or analyzed in this review article.

## 12. Acknowledgements

This work was supported by grants from the National Research Foundation of Korea (NRF) funded by the Korea government (MSIT) (RS-2023-00223831, RS-2023-00211757, RS-2026-25499888 to Munhyung Bae), National Research Foundation of Korea (NRF) funded by the Korea government (MSIT) (RS-2025-23525419), Korea Basic Science Institute (National research Facilities and Equipment Center) funded by the Korea government (MSIT) (RS-2024-00403999 to Munhyung Bae), and Korea Basic Science Institute (National research Facilities and Equipment Center) funded by the Ministry of Education (RS-2025-02308336). The research was also supported by the Global University 30 Project at Pusan National University through the Busan Regional Innovation System & Education (RISE) Project, funded by the Ministry of Education and Busan Metropolitan City, Republic of Korea. (2025-glocal-02-004-511-002).

## 13. References

- 1 D. J. Newman and G. M. Cragg, *J. Nat. Prod.*, 2020, **83**, 770–803.
- 2 W. Hou and H. Xu, *J. Med. Chem.*, 2022, **65**, 4436–4456.
- 3 M. C. Walker and M. C. Y. Chang, *Chem. Soc. Rev.*, 2014, **43**, 6527–6536.
- 4 S. Walker, R. Landovitz, W. D. Ding, G. A. Ellestad and D. Kahne, *Proc. Natl. Acad. Sci. U. S. A.*, 1992, **89**, 4608–4612.
- 5 J. M. Macho, R. M. Blue, H. W. Lee and J. B. MacMillan, *Org. Lett.*, 2022, **24**, 3161–3166.



- 6 P. J. White, *Ann. Bot.*, 2016, **117**, 217–235.
- 7 K. S. Patel, P. K. Pandey, P. Martín-Ramos, W. T. Corns, S. Varol, P. Bhattacharya and Y. Zhu, *RSC Adv.*, 2023, **13**, 14914–14929.
- 8 F. Karahan, *Front. Life Sci. Relat. Technol.*, 2022, **3**, 43–48.
- 9 T. Hou, X. Zhao, Z. Cheng, J. Wei, M. Zhu, X. Dou and N. Jiao, *Acta Pharm. Sin. B*, 2023, **14**, 1030–1076.
- 10 S. Misra, M. Boylan, A. Selvam, J. E. Spallholz and M. Björnstedt, *Nutrients*, 2015, **7**, 3536–3556.
- 11 C. Crowe, S. Molyneux, S. V. Sharma, Y. Zhang, D. S. Gkotsi, H. Connaris and R. J. M. Goss, *Chem. Soc. Rev.*, 2021, **50**, 9443–9481.
- 12 W. Chung and C. D. Vanderwal, *Angew Chem. Int. Ed. Engl.*, 2016, **55**, 4396–4434.
- 13 R. J. Grams, W. L. Santos, I. R. Scorei, A. Abad-García, C. A. Rosenblum, A. Bitá, H. Cerecetto, C. Viñas and M. A. Soriano-Ursúa, *Chem. Rev.*, 2024, **124**, 2441–2511.
- 14 N. Astrain-Redin, I. Talavera, E. Moreno, M. J. Ramírez, N. Martínez-Sáez, I. Encío, A. K. Sharma, C. Sanmartín and D. Plano, *Antioxidants*, 2023, **12**, 139.
- 15 K. D. Bauman, K. S. Butler, B. S. Moore and J. R. Chekan, *Nat. Prod. Rep.*, 2021, **38**, 2100–2129.
- 16 L. Longwitz, R. B. Leveson-Gower, H. J. Rozeboom, A. W. H. Thunnissen and G. Roelfes, *Nature*, 2024, **629**, 824–829.
- 17 Z. Li, D. Zhu and Y. Shen, *Drug Discov. Ther.*, 2018, **12**, 318–328.
- 18 V. M. Dembitsky, A. O. Terent'ev, S. V. Baranin and M. E. Gursky, *Vietnam J. Chem.*, 2025, **63**, 883–911.
- 19 C. D. Hunt and J. Trace Elem, *Exp. Med.*, 2003, **16**, 291–306.
- 20 V. M. Dembitsky, R. Smoum, A. A. Al-Quntar, H. A. Ali, I. Pergament and M. Srebnik, *Plant Sci.*, 2002, **163**, 931–942.
- 21 H.-L. Wang, R. Li, M. Zhao, Z.-Y. Wang, H. Tang, Z.-Y. Cao, G.-L. Zheng and W. Zhang, *J. Nat. Prod.*, 2023, **86**, 429–433.
- 22 P. S. Coghi, Y. Zhu, H. Xie, N. S. Hosmane and Y. Zhang, *Molecules*, 2021, **26**, 3309.
- 23 E. D. Farfán-García, A. Kilic, J. García-Machorro, M. E. Cuevas-Galindo, B. A. Rubio-Velazquez, I. H. García-Coronel, E. Estevez-Fregoso, J. G. Trujillo-Ferrara and M. A. Soriano-Ursúa, in *Viral, Parasitic, Bacterial, and Fungal Infections*, Elsevier, 2023, pp. 733–754.
- 24 H. Irschik, D. Schummer, K. Gerth, G. Höfle and H. Reichenbach, *J. Antibiot.*, 1995, **48**, 26–30.
- 25 P. Lewer, E. L. Chapin, P. R. Graupner, J. R. Gilbert and C. Peacock, *J. Nat. Prod.*, 2003, **66**, 143–145.
- 26 M. Pérez, C. Crespo, C. Schleissner, P. Rodríguez, P. Zúñiga and F. Reyes, *J. Nat. Prod.*, 2009, **72**, 2192–2194.
- 27 D. Schummer, D. Schomburg, H. Irschik, H. Reichenbach and G. Höfle, *Liebigs Ann*, 1996, **1996**, 965–969.
- 28 J. Mulzer and M. Berger, *J. Org. Chem.*, 2004, **69**, 891–898.
- 29 S. I. Elshahawi, A. E. Trindade-Silva, A. Hanora, A. W. Han, M. S. Flores, V. Vizzoni, C. G. Schrago, C. A. Soares, G. P. Concepcion and D. L. Distel, *Helv. Chim. Acta*, 2013, **110**, E295–E304.
- 30 A. Cotto-Rosario, E. Y. Miller, F. G. Fumuso, J. A. Clement, M. J. Todd and R. M. O'Connor, *Microorganisms*, 2022, **10**, 2260.
- 31 L. Chery-Karschney, R. Patrapuvich, D. G. Mudeppa, S. Kokkonda, R. Chakrabarti, P. Sriwichai, R. M. O'Connor, P. K. Rathod and J. White, *Antimicrob. Agents Chemother.*, 2024, **68**, e00684–00623.
- 32 G. D. Bowden, P. M. Reis, M. B. Rogers, R. M. B. Relat, K. A. Brayton, S. K. Wilson, B. M. Di Genova, L. J. Knoll, A. K. Tai and T. R. Ramadhar, *Int. J. Parasitol. Drugs Drug Resist.*, 2020, **14**, 1–7.
- 33 R. M. O'Connor, F. J. Nepveux V, J. Abenoja, G. Bowden, P. Reis, J. Beaushaw, R. M. Bone Relat, I. Driskell, F. Gimenez and M. W. Riggs, *PLoS Pathog.*, 2020, **16**, e1008600.
- 34 R. Hütter, W. Keller-Schien, F. Knüsel, V. Prelog, G. Rodgers Jr, P. Suter, G. Vogel, W. Voser and H. Zähler, *Helv. Chim. Acta*, 1967, **50**, 1533–1539.
- 35 J. Dunitz, D. Hawley, D. Mikloš, D. White, Y. Berlin, R. Marušić and V. Prelog, *Helv. Chim. Acta*, 1971, **54**, 1709–1713.
- 36 J. J. Lee, T. S. Chen, C.-J. Chang, C. Fenselau and H. G. Floss, *J. Antibiot.*, 1985, **38**, 1444–1446.
- 37 T. S. Chen, C.-J. Chang and H. G. Floss, *J. Org. Chem.*, 1981, **46**, 2661–2665.
- 38 T. Yao, Z. Liu, T. Li, H. Zhang, J. Liu, H. Li, Q. Che, T. Zhu, D. Li and W. Li, *Microb. Cell Fact.*, 2018, **17**, 98.
- 39 M. A. Avery, S. C. Choudhry, O. P. Dhingra, B. D. Gray, M.-c. Kang, S.-c. Kuo, T. R. Vedananda, J. D. White and A. J. Whittle, *Org. Biomol. Chem.*, 2014, **12**, 9116–9132.
- 40 S. Hanessian, D. Delorme, P. C. Tyler, G. Demailly and Y. Chapleur, *Can. J. Chem.*, 1983, **61**, 634–637.
- 41 W. Moreira, D. B. Aziz and T. Dick, *Front. Microbiol.*, 2016, **7**, 199.
- 42 J. Abenoja, A. Cotto-Rosario and R. O'Connor, *Antimicrob. Agents Chemother.*, 2021, **65**, e01278–01220.
- 43 L. P. de Carvalho, S. Groeger-Otero, A. Kreidenweiss, P. G. Kremsner, B. Mordmüller and J. Held, *Front. Cell. Infect. Microbiol.*, 2022, **11**, 802294.
- 44 J. Kohno, T. Kawahata, T. Otake, M. Morimoto, H. Mori, N. Ueba, M. Nishio, A. Kinumaki, S. Komatsubara and K. Kawashima, *Biosci. Biotechnol. Biochem.*, 1996, **60**, 1036–1037.
- 45 Y. Okami, T. Okazaki, T. Kitahara and H. Umezawa, *J. Antibiot.*, 1976, **29**, 1019–1025.
- 46 K. Sato, T. Okazaki, K. Maeda and Y. Okami, *J. Antibiot.*, 1978, **31**, 632–635.
- 47 H. Nakamura, Y. Iitaka, T. Kitahara, T. Okazaki and Y. Okami, *J. Antibiot.*, 1977, **30**, 714–719.
- 48 J. Lee, P. Dewick, C. Gorst-Allman, F. Spreafico, C. Kowal, C. Chang, A. McInnes, J. Walter, P. Keller and H. Floss, *J. Am. Chem. Soc.*, 1987, **109**, 5426–5432.
- 49 T. S. Chen, C.-J. Chang and H. G. Floss, *J. Am. Chem. Soc.*, 1981, **103**, 4565–4568.
- 50 T. Hemscheidt, M. P. Puglisi, L. K. Larsen, G. M. Patterson, R. E. Moore, J. L. Rios and J. Clardy, *J. Org. Chem.*, 1994, **59**, 3467–3471.
- 51 F. Surup, D. Chauhan, J. Niggemann, E. Bartok, J. Herrmann, M. Keck, W. Zander, M. Stadler, V. Hornung and R. Müller, *ACS Chem. Biol.*, 2018, **13**, 2981–2988.



- 52 B. L. Bassler, M. Wright and M. R. Silverman, *Mol. Microbiol.*, 1994, **13**, 273–286.
- 53 K. C. Mok, N. S. Wingreen and B. L. Bassler, *EMBO J.*, 2003, **22**, 870–881.
- 54 X. Chen, S. Schauder, N. Potier, A. Van Dorsselaer, I. Pelczer, B. L. Bassler and F. M. Hughson, *Nature*, 2002, **415**, 545–549.
- 55 Q. Li, W. Peng, J. Wu, X. Wang, Y. Ren, H. Li, Y. Peng, X. Tang and X. Fu, *Oncoimmunology*, 2019, **8**, e1626192.
- 56 Y.-C. Ji, Q. Sun, C.-Y. Fu, X. She, X.-C. Liu, Y. He, Q. Ai, L.-Q. Li and Z.-L. Wang, *Front. Cell. Infect. Microbiol.*, 2021, **11**, 694395.
- 57 X. Zeng, H. Yue, L. Zhang, G. Chen, Q. Zheng, Q. Hu, X. Du, Q. Tian, X. Zhao and L. Liang, *Int. Immunopharmacol.*, 2023, **124**, 110971.
- 58 C. Yang, A. Hassanpour, K. Ghorbanpour, S. Abdolmohammadi and E. Vessally, *RSC Adv.*, 2019, **9**, 27625–27639.
- 59 P. T. Lowe and D. O'Hagan, *Chem. Soc. Rev.*, 2023, **52**, 248–276.
- 60 D. B. Harper and D. O'Hagan, *Nat. Prod. Rep.*, 1994, **11**, 123–133.
- 61 M. F. Carvalho and R. S. Oliveira, *Crit. Rev. Biotechnol.*, 2017, **37**, 880–897.
- 62 J. S. C. Marais, *Onderstepoort J. Vet. Sci. Anim. Ind.*, 1944, **20**, 67–73.
- 63 D. O'Hagan and D. B. Harper, *J. Fluorine Chem.*, 1999, **100**, 127–133.
- 64 R. J. Mead, D. R. King and P. H. Hubach, *Oikos*, 1985, **44**, 55–60.
- 65 J. W. Clayton Jr, *J. Occup. Med.*, 1962, **4**, 262–273.
- 66 D. O'Hagan, R. Perry, J. M. Lock, J. J. M. Meyer, L. Dasaradhi and J. T. G. Hamilton, *Phytochemistry*, 1993, **33**, 1043–1045.
- 67 T. S. Kellerman, *Onderstepoort J. Vet. Res.*, 2009, **74**, 1–4.
- 68 L. E. Twigg and D. R. King, *Wildl. Res.*, 1991, **18**, 615–629.
- 69 C. Eason, A. Miller, S. Ogilvie and A. Fairweather, *N. Z. J. Ecol.*, 2011, **35**, 1–20.
- 70 C. T. Eason, *Chem. Australas.*, 2018, **85**, 62–67.
- 71 R. A. Peters and M. Shorthouse, *Nature*, 1967, **213**, 941–942.
- 72 R. A. Peters and M. Shorthouse, *Nature*, 1971, **232**, 415–416.
- 73 P. W. Chan and D. O'Hagan, *Methods Enzymol.*, 2012, **516**, 219–236.
- 74 M. F. Carvalho and D. O'Hagan, *RSC Adv.*, 2017, **7**, 13270–13285.
- 75 C. D. Murphy, C. Schaffrath and D. O'Hagan, *Appl. Environ. Microbiol.*, 2001, **67**, 4919–4922.
- 76 S. A. Sooklal, P. T. Mpangase, M.-S. Tomescu, S. Aron, S. Hazelhurst, R. H. Archer and K. Rumbold, *Sci. Rep.*, 2020, **10**, 20539.
- 77 L. E. X. Leong, S. Khan, C. K. Davis, S. E. Denman and C. S. McSweeney, *J. Anim. Sci. Biotechnol.*, 2017, **8**, 55.
- 78 M. L. Vickery and B. Vickery, *Phytochemistry*, 1972, **11**, 961–965.
- 79 J. T. G. Hamilton and D. B. Harper, *Phytochemistry*, 1997, **46**, 217–223.
- 80 D. B. Harper, J. T. G. Hamilton and D. O'Hagan, *Tetrahedron Lett.*, 1990, **31**, 2203–2206.
- 81 J. Han, L. Kiss, H. Mei, A. M. Remete, M. Ponikvar-Svet, D. M. Sedgwick, R. Roman, S. Fustero, H. Moriwaki and V. A. Soloshonok, *Chem. Rev.*, 2021, **121**, 4678–4742.
- 82 M. Sanada, T. Miyano, S. Iwadare, J. M. Williamson, B. H. Arison, J. L. Smith, A. W. Douglas, J. M. Liesch and E. Inamine, *J. Antibiot.*, 1986, **39**, 259–265.
- 83 C. Zhao, P. Li, H.-Y. Ou, R. P. McGlinchey and D. O'Hagan, *Bioorg. Chem.*, 2012, **44**, 1–7.
- 84 L. Wu and H. Deng, *Org. Biomol. Chem.*, 2020, **18**, 4462–4471.
- 85 P.-T. Lowe, *Chem. Soc. Rev.*, 2023, **52**, 865–887.
- 86 X. M. Zhu, S. Hackl, M. N. Thaker, L. Kalan, C. Weber, D. S. Urgast, E. M. Krupp, A. Brewer, S. Vanner, A. Szawiola, G. Yim, J. Feldmann, A. Bechthold, G. D. Wright and D. L. Zechel, *ChemBioChem*, 2015, **16**(17), 2498–2506.
- 87 A. R. O. Pasternak, A. Bechthold and D. L. Zechel, *ChemBioChem*, 2022, **23**, e202200140.
- 88 D. A. Shuman, M. J. Robins and R. K. Robins, *J. Am. Chem. Soc.*, 1969, **91**, 2639–2640.
- 89 S. O. Thomas, V. L. Singleton, J. A. Lowery, R. W. Sharpe, L. M. Pruess, J. N. Porter, J. H. Mowat and N. Bohonos, *US Pat.*, 2914525, 1959.
- 90 H. Deng, C. Schaffrath and D. O'Hagan, *Nat. Prod. Rep.*, 2005, **22**, 322–342.
- 91 D. A. M. Alexandrino, I. Ribeiro, L. M. Pinto, R. Cambra, R. S. Oliveira, F. Pereira and M. F. Carvalho, *N. Biotechnol.*, 2018, **43**, 23–29.
- 92 S. Muzaffar, J. Khan, R. Srivastava, M. S. Gorbatyuk and M. Athar, *Cell Biol. Toxicol.*, 2023, **39**, 85–110.
- 93 W. R. Cullen and K. J. Reimer, *Chem. Rev.*, 1989, **89**, 713–764.
- 94 R. Bentley and T. G. Chasteen, *Microbiol. Mol. Biol. Rev.*, 2002, **66**, 250–271.
- 95 K. Shiomi, A. Shinagawa, K. Hirota, H. Yamanaka and T. Kikuchi, *Agric. Biol. Chem.*, 1984, **48**, 2863–2864.
- 96 C. Eason, A. Miller, S. Ogilvie and A. Fairweather, *Environ. Sci.: Processes Impacts*, 2013, **15**, 1552–1562.
- 97 A. Popowich, Q. Zhang and X. C. Le, *Natl. Sci. Rev.*, 2016, **3**, 451–458.
- 98 X.-M. Xue, J. Ye, G. Raber, B. P. Rosen, K. Francesconi, C. Xiong, Z. Zhu, C. Rensing and Y.-G. Zhu, *Environ. Sci. Technol.*, 2019, **53**, 634–641.
- 99 K. A. Francesconi, *Pure Appl. Chem.*, 2010, **82**, 373–381.
- 100 T. Hoffmann, B. Warmbold, S. H. J. Smits, B. Tschapek, S. Ronzheimer, A. Bashir, C. Chen, A. Rolbetzki, M. Pittelkow, M. Jebbar, A. Seubert, L. Schmitt and E. Bremer, *Environ. Microbiol.*, 2018, **20**, 305–323.
- 101 V. Taylor, B. Goodale, A. Raab, T. Schwerdtle, K. Reimer, S. Conklin, M. R. Karagas and K. Francesconi, *A. Sci. Total Environ.*, 2017, **580**, 266–282.
- 102 C. Luvonga, C. A. Rimmer, L. L. Yu and S. B. Lee, *J. Agric. Food Chem.*, 2020, **68**, 943–960.
- 103 EFSA Panel on Contaminants in the Food Chain (CONTAM), Scientific opinion on arsenic in food, *EFSA J.*, 2009, **7**, 1351.



- 104 S. Fukuda, M. Terasawa and K. Shiomi, *Food Chem. Toxicol.*, 2011, **49**, 1598–1603.
- 105 A. D. Welch and R. L. Landau, *J. Biol. Chem.*, 1942, **144**, 581–588.
- 106 V. Sele, J. J. Sloth, A.-K. Lundebye, E. H. Larsen, M. H. G. Berntssen and H. Amlund, *Food Chem.*, 2012, **133**, 618–630.
- 107 S. A. Viczek, K. B. Jensen and K. A. Francesconi, *Angew. Chem., Int. Ed.*, 2016, **55**, 5259–5262.
- 108 K. Shiomi, M. Chino and T. Kikuchi, *Appl. Organomet. Chem.*, 1990, **4**, 281–286.
- 109 S. Meyer, M. Matissek, S. M. Müller, M. S. Taleshi, F. Ebert, K. A. Francesconi and T. Schwerdtle, *Metallomics*, 2014, **6**, 1023–1033.
- 110 I. Mancini, G. Guella, M. Frostin, E. Hnawia, D. Laurent, C. Debitus and F. Pietra, *Chem.–Eur. J.*, 2006, **12**(35), 8989–8994.
- 111 T. Chávez-Capilla, *DNA Cell Biol.*, 2022, **41**(1), 64–70.
- 112 D. Lu, M. L. Coote, J. Ho, N. L. Kilah, C.-Y. Lin, G. Salem, M. L. Weir, A. C. Willis, P. J. Dilda and S. B. Wild, *Organometallics*, 2012, **31**, 1808–1816.
- 113 P. Tähtinen, G. Guella, G. Saielli, C. Debitus, E. Hnawia and I. Mancini, *Mar. Drugs*, 2018, **16**(10), 382.
- 114 J. Chen and B. P. Rosen, *Front. Environ. Sci.*, 2020, **8**, 43.
- 115 V. S. Nadar, J. Chen, D. S. Dheeman, A. E. Galván, K. Yoshinaga-Sakurai, P. Kandavelu, B. Sankaran, M. Kuramata, S. Ishikawa, B. P. Rosen and M. Yoshinaga, *Commun. Biol.*, 2019, **2**, 131.
- 116 B. Moe, H. Peng, X. Lu, B. Chen, L. W. L. Chen, S. Gabos, X.-F. Li and X. C. Le, *J. Environ. Sci.*, 2016, **49**, 113–124.
- 117 V. M. Dembitsky, A. O. Terent'ev, M. E. Gursky and S. V. Baranin, *Vietnam J. Chem.*, 2025, **63**(2), 1–29.
- 118 G. Genchi, G. Lauria, A. Catalano, M. S. Sinicropi and A. Carocci, *Int. J. Mol. Sci.*, 2023, **24**, 2633.
- 119 M. Roman, P. Jitaru and C. Barbante, *Metallomics*, 2014, **6**, 25–54.
- 120 C. M. Kayrouz, J. Huang, N. Hauser and M. R. Seyedsayamdost, *Nature*, 2022, **610**, 199–204.
- 121 H. Achibat, N. A. AlOmari, F. Messina, L. Sancineto, M. Khouili and C. Santi, *Nat. Prod. Commun.*, 2015, **10**, 1934578X1501001119.
- 122 C. Gallo-Rodriguez and J. B. Rodriguez, *ChemMedChem*, 2024, **19**, e202400063.
- 123 Y. Yamashita, T. Yabu and M. Yamashita, *World J. Biol. Chem.*, 2010, **1**, 144.
- 124 N. G. Turrini, N. Kroepfl, K. B. Jensen, T. C. Reiter, K. A. Francesconi, T. Schwerdtle, W. Kroutil and D. Kuehnelt, *Metallomics*, 2018, **10**, 1532–1538.
- 125 C. M. Kayrouz and M. R. Seyedsayamdost, *bioRxiv*, 2022, 2022–2004.
- 126 T. Seko, Y. Yamashita and M. Yamashita, *Metallomics Res*, 2025, **5**, rev24–rev35.
- 127 T. Seko, S. Imamura, K. Ishihara, Y. Yamashita and M. Yamashita, *Fish. Sci.*, 2020, **86**, 171–179.
- 128 V. M. Labunskyy, D. L. Hatfield and V. N. Gladyshev, *Physiol. Rev.*, 2014, **94**, 739–777.
- 129 M. C. Escobar-Ramírez, G. M. Rodríguez-Serrano, E. Zúñiga-León, M. A. García-Montes, E. Pérez-Escalante and L. G. González-Olivares, *Fermentation*, 2023, **9**, 684.
- 130 C.-d. Fan, X.-y. Fu, Z.-y. Zhang, M.-z. Cao, J.-y. Sun, M.-f. Yang, X.-t. Fu, S.-j. Zhao, L.-r. Shao and H.-f. Zhang, *Sci. Rep.*, 2017, **7**, 6465.
- 131 S. H. Kim, B. K. Kim and S. K. Park, *Mol. Med. Rep.*, 2018, **18**, 5389–5398.
- 132 L. B. Maia, B. K. Maiti, I. Moura and J. J. G. Moura, *Molecules*, 2023, **29**, 120.
- 133 C. M. Kayrouz, K. A. Ireland, V. Y. Ying, K. M. Davis and M. R. Seyedsayamdost, *Nat. Chem.*, 2024, **16**, 1868–1875.
- 134 V. M. Dembitsky, *Nat. Prod. Commun.*, 2006, **1**, 1934578X0600100210.
- 135 H. Al-Adilah, M. C. Feiters, L. J. Carpenter, P. Kumari, C. J. Carrano, D. Al-Bader and F. C. Kupper, *Phycology*, 2022, **2**, 132–171.
- 136 H. Ludewig, S. Molyneux, S. Ferrinho, K. Guo, R. Lynch, D. S. Gkotsi and R. J. M. Goss, *Curr. Opin. Struct. Biol.*, 2020, **65**, 51–60.
- 137 S.-C. Lee, G. A. Williams and G. D. Brown, *Phytochem.*, 1999, **52**, 537–540.
- 138 K. Dabrovolskas, I. Jonuškienė, S. Sutkuvienė and D. Gudeika, *Chemija*, 2020, 31.
- 139 T. Wang, P. Rabe, C. A. Citron and J. S. Dickschat, *Beilstein J. Org. Chem.*, 2013, **9**, 2767–2777.
- 140 T. Iizuka, R. Fudou, Y. Jojima, S. Ogawa, S. Yamanaka, Y. Inukai and M. Ojika, *J. Antibiot.*, 2006, **59**, 385–391.
- 141 Y. Liu, S. Yamazaki and M. Ojika, *Molecules*, 2023, **28**, 2815.
- 142 M. Ojika, Y. Inukai, Y. Kito, M. Hirata, T. Iizuka and R. Fudou, *Chem.–Asian J.*, 2008, **3**, 126–133.
- 143 P. G. Williams, W. Y. Yoshida, R. E. Moore and V. J. Paul, *Org. Lett.*, 2003, **5**, 4167–4170.
- 144 Y. Chen, W. Yang, G. Zou, G. Wang, W. Kang, J. Yuan and Z. She, *J. Nat. Prod.*, 2022, **85**, 1229–1238.
- 145 B.-C. Yan, W.-G. Wang, D.-B. Hu, X. Sun, T. Kong, Y. Wang, H. Sun, H.-Y. Li, J.-J. Dai, D.-Q. Luo, J.-G. Luo, X.-J. Hao and X.-L. Li, *Org. Lett.*, 2016, **18**, 1108–1111.
- 146 Y.-F. Luo, M. Zhang, J.-G. Dai, P. Pedpradab, W.-J. Wang and J. Wu, *Phytochem. Lett.*, 2016, **17**, 162–166.
- 147 R. Chen, L. Guo, X. Li, X. Li, K. Hu, J. Tang, Z. Ye, B. Yan and P. Puno, *Org. Chem. Front.*, 2023, **10**, 2218–2225.
- 148 M. D. Lee, J. K. Manning, D. R. Williams, N. A. Kuck, R. T. Testa and D. B. Borders, *J. Antibiot.*, 1989, **42**, 1070–1087.
- 149 S. G. Van Lanen and B. Shen, *Curr. Top. Med. Chem.*, 2008, **8**, 448–459.
- 150 B. Zhao, S. Konno, J. M. Wu and A. L. Oronsky, *Cancer Lett.*, 1990, **50**, 141–147.
- 151 D. A. Dias, K. A. Kouremenos, D. J. Beale, D. L. Callahan and O. A. H. Jones, *BioMetals*, 2016, **29**, 1–13.
- 152 C. E. Valdez, Q. A. Smith, M. R. Nechay and A. N. Alexandrova, *Acc. Chem. Res.*, 2014, **47**, 3110–3117.
- 153 D. Rehder, in *Interrelations between Essential Metal Ions and Human Diseases*, ed. A. Sigel, H. Sigel and R. K. O. Sigel, Springer, Dordrecht, 2013, pp. 139–169.



- 154 J.-H. Huang, F. Huang, L. Evans and S. Glasauer, *Chem. Geol.*, 2015, **417**, 68–89.
- 155 S. Treviño and A. Diaz, *J. Inorg. Biochem.*, 2020, **208**, 111094.
- 156 D. Rehder, *Dalton Trans.*, 2013, **42**, 11749–11761.
- 157 D. Rehder, *Inorganica Chim. Acta*, 2020, **504**, 119445.
- 158 E. Bayer and H. Kneifel, *Z. Naturforsch. B J. Chem. Sci.*, 1972, **27**, 207.
- 159 T. Ueki, T. Adachi, S. Kawano, M. Aoshima, N. Yamaguchi, K. Kanamori and H. Michibata, *Biochim. Biophys. Acta*, 2003, **1626**, 43–50.
- 160 H. Vilter, K.-W. Glombitza and A. Grawe, *Bot. Mar.*, 1983, **26**, 331–340.
- 161 H. Kneifel and E. Bayer, *Angew Chem. Int. Ed. Engl.*, 1973, **12**, 508.
- 162 C. D. Garner, E. M. Armstrong, R. E. Berry, R. L. Beddoes, D. Collison, J. J. Cooney, S. N. Ertok and M. Helliwell, *J. Inorg. Biochem.*, 2000, **80**, 17–20.
- 163 J. A. L. da Silva, J. J. R. Fraústo da Silva and A. J. L. Pombeiro, *Coord. Chem. Rev.*, 2013, **257**, 2388–2400.
- 164 J. J. R. Fraústo da Silva, *Chem. Speciat. Bioavail.*, 1989, **1**, 139–150.
- 165 C. M. M. Matoso, A. J. L. Pombeiro, J. J. R. Fraústo da Silva, M. F. C. G. da Silva, J. A. L. da Silva, J. L. Baptista-Ferreira and F. Pinho-Almeida, in *Vanadium Compounds*, American Chemical Society, 1998, 711, pp. 241–247.
- 166 M. Domarus, M. L. Kuznetsov, J. Marçalo, A. J. L. Pombeiro and J. A. L. da Silva, *Angew Chem. Int. Ed. Engl.*, 2016, **55**, 1489–1492.
- 167 R. E. Berry, E. M. Armstrong, R. L. Beddoes, D. Collison, S. N. Ertok, M. Helliwell and C. D. Garner, *Angew Chem. Int. Ed. Engl.*, 1999, **38**, 795–797.
- 168 E. M. Armstrong, D. Collison, N. Ertok and C. D. Garner, *Talanta*, 2000, **53**, 75–87.
- 169 P. M. Reis, J. Armando, L. Silva, J. J. R. F. da Silva and A. J. L. Pombeiro, *Chem. Commun.*, 2000, 1845–1846.
- 170 M. F. C. Guedes da Silva, J. A. L. da Silva, J. J. R. Fraústo da Silva, A. J. L. Pombeiro, C. Amatore and J.-N. Verpeaux, *J. Am. Chem. Soc.*, 1996, **118**, 7568–7573.
- 171 P. M. Reis, J. A. L. Silva, A. F. Palavra, J. J. R. Fraústo da Silva, T. Kitamura, Y. Fujiwara and A. J. L. Pombeiro, *Angew Chem. Int. Ed. Engl.*, 2003, **42**, 821–823.
- 172 T. Kanda, Y. Nose, J. Wuchiyama, T. Uyama, Y. Moriyama and H. Michibata, *Zool. Sci.*, 1997, **14**, 37–42.
- 173 T. Ishii, T. Otake, K. Okoshi, M. Nakahara and R. Nakamura, *Mar. Biol.*, 1994, **121**, 143–151.
- 174 J. Wuchiyama, Y. Nose, T. Uyama and H. Michibata, *Zool. Sci.*, 1997, **14**, 409–414.
- 175 K. Fukui, T. Ueki, H. Ohya and H. Michibata, *J. Am. Chem. Soc.*, 2003, **125**, 6352–6353.
- 176 T. Hamada, M. Asanuma, T. Ueki, F. Hayashi, N. Kobayashi, S. Yokoyama, H. Michibata and H. Hirota, *J. Am. Chem. Soc.*, 2005, **127**, 4216–4222.
- 177 M. Weyand, H.-J. Hecht, M. Kieß, M.-F. Liaud, H. Vilter and D. Schomburg, *J. Mol. Biol.*, 1999, **293**, 595–611.
- 178 T. Ueki, T. Uyama, K. Yamamoto, K. Kanamori and H. Michibata, *Biochim. Biophys. Acta*, 2000, **1494**, 83–90.
- 179 J. W. Van Schijndel, P. Barnett, J. Roelse, E. G. Vollenbroek and R. Wever, *Eur. J. Biochem.*, 1994, **225**, 151–157.
- 180 A. A. Brindley, A. R. Dalby, M. N. Isupov and J. A. Littlechild, *Acta. Crystallogr. D Biol. Crystallogr.*, 1998, **54**, 454–457.
- 181 H. Plat, B. E. Krenn and R. Wever, *Biochem. J.*, 1987, **248**, 277–279.
- 182 R. L. Robson, R. R. Eady, T. H. Richardson, R. W. Miller, M. Hawkins and J. R. Postgate, *Nature*, 1986, **322**, 388–390.
- 183 R. R. Eady, *Coord. Chem. Rev.*, 2003, **237**, 23–30.
- 184 C. C. Lee, Y. Hu and M. W. Ribbe, *Science*, 2010, **329**, 642.
- 185 H. Bortels, *Archiv. Mikrobiol.*, 1930, **1**, 333–342.
- 186 R. Hille, *Chem. Rev.*, 1996, **96**, 2757–2816.
- 187 E. I. Stiefel, *Met. Ions. Biol. Syst.*, 2002, **39**, 1–29.
- 188 R. R. Mendel and F. Bittner, *Biochim. Biophys. Acta Mol. Cell. Res.*, 2006, **1763**, 621–635.
- 189 R. R. Mendel, *Dalton Trans.*, 2005, 3404–3409.
- 190 G. Schwarz and R. R. Mendel, *Annu. Rev. Plant Biol.*, 2006, **57**, 623–647.
- 191 C. Enroth, B. T. Eger, K. Okamoto, T. Nishino, T. Nishino and E. F. Pai, *Proc. Natl. Acad. Sci. U. S. A.*, 2000, **97**, 10723–10728.
- 192 C. Kisker, H. Schindelin, A. Pacheco, W. A. Wehbi, R. M. Garrett, K. V. Rajagopalan, J. H. Enemark and D. C. Rees, *Cell*, 1997, **91**, 973–983.
- 193 K. Fischer, G. G. Barbier, H.-J. Hecht, R. R. Mendel, W. H. Campbell and G. Schwarz, *Plant Cell*, 2005, **17**(1), 1167–1179.
- 194 G. Lu, Y. Lindqvist, G. Schneider, U. Dwivedi and W. Campbell, *J. Mol. Biol.*, 1995, **248**, 931–948.
- 195 J. Kim and D. C. Rees, *Science*, 1992, **257**, 1677–1682.
- 196 J. L. Johnson, H. J. Cohen and K. V. Rajagopalan, *J. Biol. Chem.*, 1974, **249**, 5046–5055.
- 197 J. L. Johnson, B. E. Hainline and K. V. Rajagopalan, *J. Biol. Chem.*, 1980, **255**, 1783–1786.
- 198 S. P. Cramer, R. Wahl and K. V. Rajagopalan, *J. Am. Chem. Soc.*, 1981, **103**, 7721–7727.
- 199 C. Kisker, H. Schindelin and D. C. Rees, *Annu. Rev. Biochem.*, 1997, **66**, 233–267.
- 200 M. Duran, F. A. Beemer, C. van de Heiden, J. Korteland, P. K. de Bree, M. Brink, S. K. Wadman and I. Lombeck, *J. Inherit. Metab. Dis.*, 1978, **1**, 175–178.
- 201 J. Reiss, *Hum. Genet.*, 2000, **106**, 157–163.
- 202 J. Reiss and J. L. Johnson, *Hum. Mutat.*, 2003, **21**, 569–576.
- 203 B. K. Burgess and D. J. Lowe, *Chem. Rev.*, 1996, **96**, 2983–3012.
- 204 J. B. Howard and D. C. Rees, *Chem. Rev.*, 1996, **96**, 2965–2982.
- 205 O. Einsle, F. A. Tezcan, S. L. A. Andrade, B. Schmid, M. Yoshida, J. B. Howard and D. C. Rees, *Science*, 2002, **297**, 1696–1700.
- 206 T. Spatzal, M. Aksoyoglu, L. Zhang, S. L. A. Andrade, E. Schleicher, S. Weber, D. C. Rees and O. Einsle, *Science*, 2011, **334**, 940.
- 207 L. C. Seefeldt, B. M. Hoffman and D. R. Dean, *Annu. Rev. Biochem.*, 2009, **78**, 701–722.

